NeuroImage 146 (2017) 642–657

Contents lists available at ScienceDirect

NeuroImage

journal homepage: www.elsevier.com/locate/neuroimage

The tuning of human visual cortex to variations in the $1/f^{\alpha}$ amplitude spectra and fractal properties of synthetic noise images

Zoey J. Isherwood[a,b,*], Mark M. Schira[b,c], Branka Spehar[a,*]

[a] School of Psychology, UNSW Australia, Sydney, NSW 2052, Australia
[b] Neuroscience Research Australia, Randwick, NSW 2031, Australia
[c] School of Psychology, University of Wollongong, Wollongong, NSW 2522, Australia

ARTICLE INFO

Keywords:
fMRI
Vision
Fractals
Natural scene statistics
1/f amplitude spectrum

ABSTRACT

Natural scenes share a consistent distribution of energy across spatial frequencies (SF) known as the $1/f^{\alpha}$ amplitude spectrum ($\alpha \approx 0.8–1.5$, mean 1.2). This distribution is scale-invariant, which is a fractal characteristic of natural scenes with statistically similar structure at different spatial scales. While the sensitivity of the visual system to the 1/f properties of natural scenes has been studied extensively using psychophysics, relatively little is known about the tuning of cortical responses to these properties. Here, we use fMRI and retinotopic mapping techniques to measure and analyze BOLD responses in early visual cortex (V1, V2, and V3) to synthetic noise images that vary in their $1/f^{\alpha}$ amplitude spectra (α=0.25 to 2.25, step size: 0.50) and contrast levels (10% and 30%) (Experiment 1). To compare the dependence of the BOLD response between the photometric (intensity based) and geometric (fractal) properties of our stimuli, in Experiment 2 we compared grayscale noise images to their binary (thresholded) counterparts, which contain only black and white regions. In both experiments, early visual cortex responded maximally to stimuli generated to have an input 1/f slope corresponding to natural $1/f^{\alpha}$ amplitude spectra, and lower BOLD responses were found for steeper or shallower 1/f slopes (peak modulation: 0.59% for 1.25 vs. 0.31% for 2.25). To control for changing receptive field sizes, responses were also analyzed across multiple eccentricity bands in cortical surface space. For most eccentricity bands, BOLD responses were maximal for natural $1/f^{\alpha}$ amplitude spectra, but importantly there was no difference in the BOLD response to grayscale stimuli and their corresponding thresholded counterparts. Since the thresholding of an image changes its measured 1/f slope (α) but not its fractal characteristics, this suggests that neuronal responses in early visual cortex are not strictly driven by spectral slope values (photometric properties) but rather their embedded geometric, fractal-like scaling properties.

1. Introduction

Natural scenes share a surprising number of statistical regularities despite vast differences in their appearance (i.e. beaches, forests, and canyons). One of the most notable statistical regularities present in nature is the $1/f^{\alpha}$ amplitude spectrum, which describes a distribution of energy across spatial frequencies (SF). This distribution falls on a line when plotted on a log scale, and the slope of this line is referred to as the 1/f slope (α) which is typically around 0.8 to 1.5 (mean=1.2) for natural scenes (Tolhurst et al., 1992). Natural $1/f^{\alpha}$ amplitude spectra are also scale-invariant, and as such natural scenes are considered fractal – containing a similar amount and distribution of structure across different spatial scales. A number of studies have demonstrated that the visual system is tuned to the $1/f^{\alpha}$ amplitude spectrum and is best able to discriminate images with a 1/f slope (α) within the natural range ($\alpha \approx 1.2–1.4$) compared to images with 1/f slopes outside of this range (Hansen and Hess, 2006; Knill et al., 1990; Tadmor and Tolhurst, 1994). While the tuning toward the $1/f^{\alpha}$ amplitude spectrum has been demonstrated psychophysically, the neuronal processes underlying this optimization remain unclear.

There are many computational theories that predict the visual system's neuronal response magnitude to the $1/f^{\alpha}$ amplitude spectrum, however their predictions are conflicting. For instance, response equalization theory predicts equalized activation across all SF selective

Abbreviations: ANOVA, analysis of variance; AR, aesthetic rating; BOLD, blood oxygen level dependent; CVS, central visual search; D, fractal dimension; EPI, echo planar image; FFT, fast Fourier transform; fMRI, functional magnetic resonance imaging; FOV, field of view; GLM, general linear model; HRF, hemodynamic response function; MPRAGE, magnetization-prepared rapid acquisition with gradient echo; RCS, rectified contrast spectrum; RMS, root mean square; ROI, region of interest; SENSE, sensitivity encoding; SF, spatial frequency; SPM, statistical parametric mapping; TE, echo time; TR, repetition time

* Corresponding authors at: School of Psychology, UNSW Australia, Sydney, NSW 2052, Australia.
E-mail address: z.isherwood@student.unsw.edu.au (Z.J. Isherwood).

http://dx.doi.org/10.1016/j.neuroimage.2016.10.013
Received 11 May 2016; Accepted 8 October 2016
Available online 11 October 2016

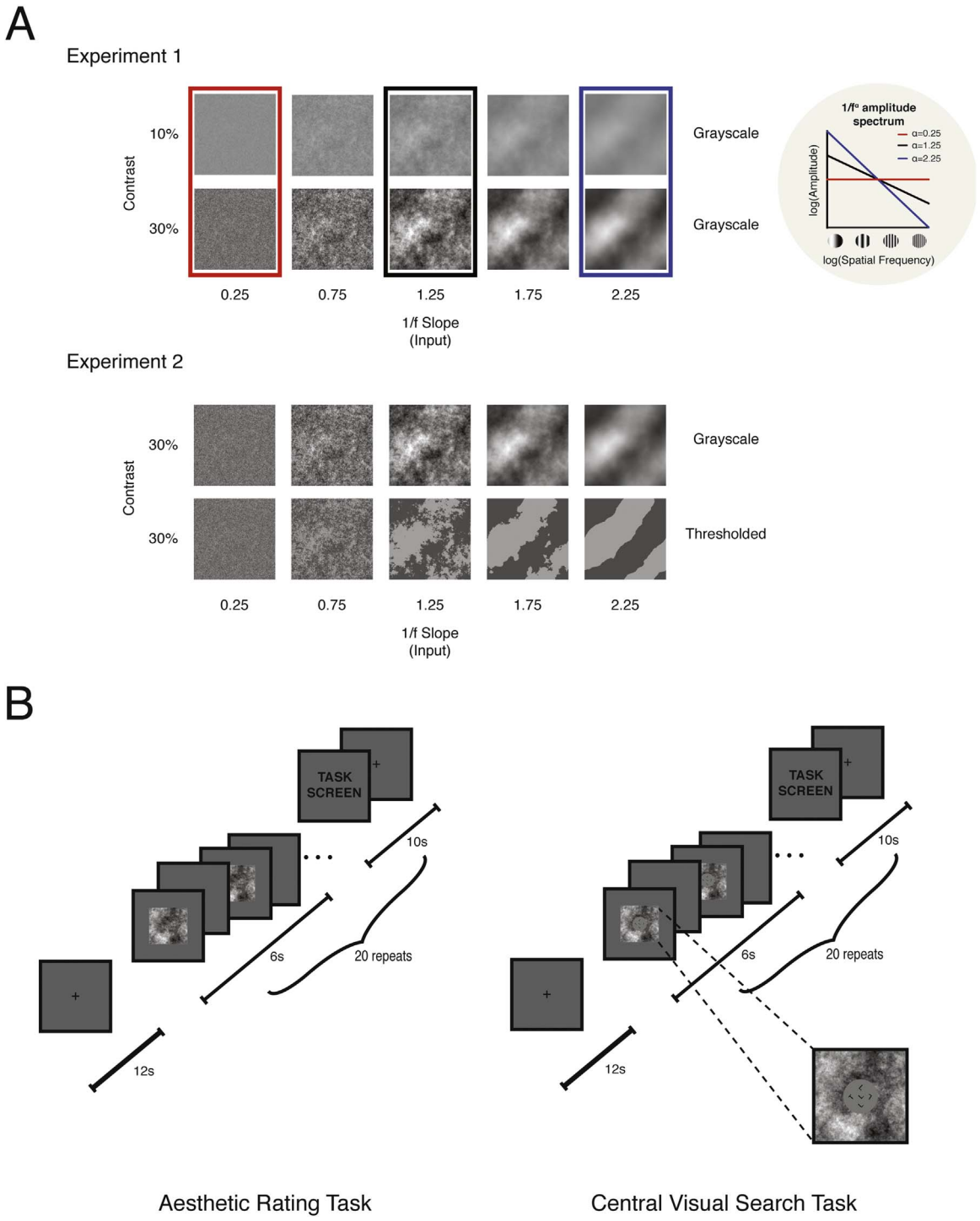

Fig. 1. Stimuli and experimental conditions used in Experiment 1 and 2. A) Examples of the images used across Experiment 1 and Experiment 2. The images in Experiment 1 consisted of grayscale synthetic noise images at 10% contrast (top row) and 30% contrast (bottom row) across a range of 1/f slopes. The images in Experiment 2 consisted of grayscale (top row) and thresholded (bottom row) synthetic noise images at 30% contrast across a range of 1/f slopes. B) Block design used in both Experiment 1 and Experiment 2. The same task conditions were employed in both experiments: 1) Aesthetic Rating (AR) where subjects had to indicate their overall preference of each block of images on a Likert scale ranging from 1 to 4 (Strongly Dislike, Somewhat Dislike, Somewhat Like, and Strongly Like), and 2) Central Visual Search (CVS) where subjects had to indicate how many target letters in total were presented in each block, which ranged from 1 to 4.

neurons (Brady and Field, 1995; Field and Brady, 1997) while sparse coding theory predicts only a few neurons to be active so the least amount of energy is expended (Barlow, 1972; Field, 1987, 1994). Evidence from previous fMRI studies has demonstrated that overall responses in early visual cortex are highest for images that have natural $1/f^{\alpha}$ amplitude spectra (Olman et al., 2004; Rieger et al., 2013). This finding can be considered in line with the theory of response equalization (Brady and Field, 1995; Field and Brady, 1997) since sparse coding predicts the opposite finding – that is, minimal neuronal responses for stimuli with a natural 1/f slope and stronger responses for stimuli with a 1/f slope outside the natural range.

Despite these findings, it is possible that the conclusions about the tuning of the visual system to $1/f^{\alpha}$ amplitude spectra from Olman et al. (2004) and Rieger et al. (2013) are premature. Firstly, responses were

Table 1
Comparison of measured 1/f slope and fractal dimension across grayscale and thresholded image types.

		Image type	
	Input 1/f Slope	Grayscale	Thresholded
Measured 1/f Slope (α)	0.25	0.25 (0.03)	0.20 (0.03)
	0.75	0.76 (0.03)	0.69 (0.03)
	1.25	1.28 (0.03)	1.09 (0.03)
	1.75	1.80 (0.03)	1.36 (0.03)
	2.25	2.10 (0.02)	1.49 (0.03)
Measured Fractal Dimension (*D*)	0.25	2.10 (0.03)	2.10 (0.03)
	0.75	1.95 (0.01)	1.95 (0.01)
	1.25	1.59 (0.04)	1.59 (0.04)
	1.75	1.12 (0.06)	1.12 (0.06)
	2.25	0.86 (0.03)	0.86 (0.03)

Notes: Reported values were averaged across 30 images for each 1/f Slope condition and Image Type. Values in parentheses indicate the standard deviation.

only measured across a limited range of 1/f slopes (α=0 or 1), so it may be possible that steeper 1/f slopes. (i.e. α=2) may elicit higher neuronal responses since they have higher spatial correlations between pixels (Rikhye and Sur, 2015). Secondly, it remains unclear how responses toward the $1/f^{\alpha}$ amplitude spectrum is modulated across eccentricity ranges as it is well known that receptive field sizes change with eccentricity. This is apparent at foveal eccentricity ranges which have preferential tuning toward high SFs while peripheral eccentricity ranges have preferential tuning toward low SFs (Daniel and Whitteridge, 1961; De Valois et al., 1982; Henriksson et al., 2008; Sasaki et al., 2001; Talbot and Marshall, 1941). There is also limited theoretical and empirical work investigating the extent to which the visual system is tuned to the associated fractal, scale-invariant properties of the $1/f^{\alpha}$ amplitude spectrum. For instance, most of the variability in $1/f^{\alpha}$ amplitude spectra across natural scenes can be accounted for by the amplitude of structure across different spatial scales (photometric properties), whereas the corresponding density of structure (geometric properties) remains relatively stable (Field and Brady, 1997).

To address these points, we conducted two experiments. In Experiment 1, we measured the BOLD response to synthetic noise stimuli across two contrast levels (10% and 30%) and a wide range of 1/f slopes (α=0.25, 0.75, 1.25, 1.75, 2.25). In Experiment 2, with a new group of subjects we compared BOLD responses to grayscale synthetic noise stimuli (identical to those used in Experiment 1) to their thresholded (black and white) counterparts, again across the same range of 1/f slopes as Experiment 1 (α=0.25, 0.75, 1.25, 1.75, 2.25). Thresholding an image changes its spectral distribution, and hence its 1/f slope (α). However, while the visual appearance and photometric properties change, both grayscale and thresholded image types share the same fractal scaling characteristics as measured using a box count fractal dimension analysis (Spehar and Taylor, 2013). To investigate the effect of changing receptive field size we analyzed responses across a range of eccentricities (0.5° to 3.89°) using retinotopic mapping and surface based analyses.

2. Materials and methods

2.1. Subjects

22 healthy subjects (aged 21–24 years, 9 female) with normal or corrected-to-normal vision participated in this study. 12 subjects were recruited in Experiment 1, and 10 subjects were recruited in Experiment 2. In Experiment 1, one subject exhibited excessive head movement during scanning, and was hence removed from subsequent data analysis. Ethics approval was provided by the University of New South Wales Human Research Advisory Panel (Reference Number HC13194).

2.2. Visual display

Images were generated using MATLAB software (MathWorks) and Psychophysics Toolbox functions (Brainard, 1997; Pelli, 1997) and presented on a shielded 19 in. LCD screen located behind the scanner at a resolution of 1024×768. Subjects viewed the screen using a mirror mounted on the head coil at a viewing distance of 1.5 m, resulting in a display spanning 11° in visual angle (or 5.50° in eccentricity).

2.3. Stimuli

2.3.1. Experiment 1: 1/f slope and contrast manipulation

Synthetic noise images were generated using a custom MATLAB code that allows precise control of the distribution of pixel intensities (1/f slope) and root mean squared (RMS) contrast. Each stimulus was created starting from a random distribution of pixel intensities, Fourier transforming this distribution, and then adjusting the component SFs to conform to an amplitude spectrum proportional to $1/f^{\alpha}$. Images were generated at five different input α values (0.25, 0.75, 1.25, 1.75, and 2.25) and two different contrast levels (10% and 30%) at a size of 512×512 pixels, which subtended 7.36° visual angle (Fig. 1A, top panel). When generating stimuli with a specific input α value there is some discrepancy between input and output α value caused by rounding to the nearest 8-bit integer (see Table 1). However, this difference is negligible and as such all terminology referring to the 1/f slope will refer to the input α value unless otherwise stated.

2.3.2. Experiment 2: Grayscale vs. Thresholded image manipulation

The grayscale images used in this experiment were generated identically to Experiment 1 using the same range of input α values. The RMS contrast of the grayscale images was 30%, identical to the high contrast condition in Experiment 1. The corresponding thresholded images were created by thresholding each grayscale image at mean luminance. For example, if pixel intensity ranges between 0 and 1 in a given image, and the mean luminance of the image is 0.5, any pixel value below 0.5 is assigned a value of 0 and anything above 0.5 is assigned a value of 1, resulting in a two toned black and white image (Fig. 1A, bottom panel).

To ensure both grayscale and thresholded images had the same mean luminance (127.50, *SD*=38.23) and mean RMS contrast level (30%), the lumMatch function from the SHINE toolbox was used to match these two properties across all generated images (Willenbockel et al., 2010). The lumMatch function of the SHINE toolbox works by initially measuring the mean luminance of a stimulus set, and then setting the mean luminance of each image to the mean luminance of the set (Willenbockel et al., 2010). The luminance distribution between images is not matched in this procedure, but is scaled to ensure the mean luminance of each image is the same as the mean luminance of the set (Fig. 2). See Tables 1 and 2 of the Supplementary Materials for a list of measured luminance and RMS contrast values before and after the lumMatch function was used across the stimulus set.

2.4. Image analysis

2.4.1. Effect of thresholding on the $1/f^{\alpha}$ amplitude spectrum

In Experiment 2, we investigated the dependence of the BOLD response on the photometric and the geometric image characteristics of our synthetic noise images by comparing our original grayscale images with their thresholded (black and white) counterparts. The input 1/f slopes used to generate stimuli across the two image type conditions (grayscale and thresholded) were the same. However, as a consequence of the thresholding procedure, the measured 1/f slopes of thresholded stimuli differ from their original grayscale counterparts from which

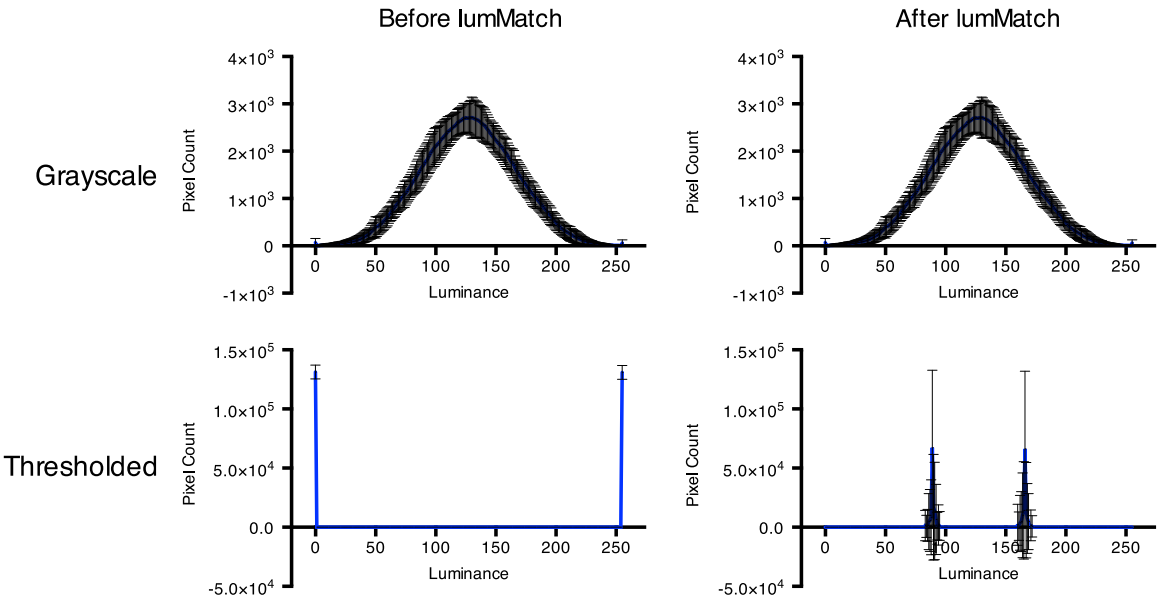

Fig. 2. Luminance distributions before and after the lumMatch function was used. Data plotted are the average luminance distributions of all grayscale (top row) and thresholded (bottom row) stimuli used in Experiment 2. The lumMatch function of the SHINE toolbox (Willenbockel et al., 2010) was used to equate both grayscale (top row) and thresholded (bottom row) stimuli in their mean luminance. The luminance distributions across all stimuli were not matched, but were scaled in order to ensure each image had the same mean luminance. For a list of luminance distributions for each image type, see Tables 1 and 2 of the Supplementary Materials.

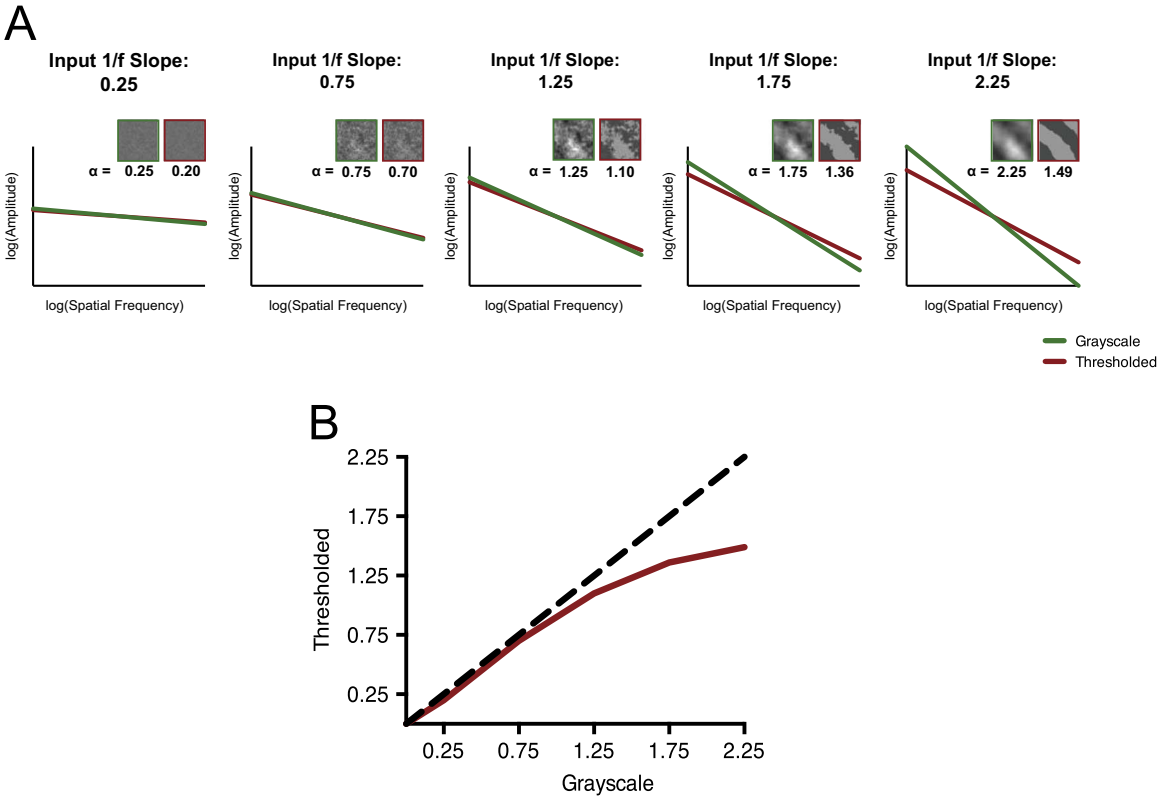

Fig. 3. Comparison of the $1/f^{\alpha}$ amplitude spectrum between grayscale and thresholded noise stimuli. A) Linear fit of the $1/f^{\alpha}$ amplitude spectra on a log scale plotted for each 1/f slope condition across both image types: grayscale (green) and thresholded (red). From shallow 1/f slope conditions (i.e. 0.25) to steeper 1/f slope conditions (2.25), the 1/f slope for thresholded images becomes shallower compared to their grayscale counterparts. B) A plot comparing the measured 1/f slope of grayscale (x-axis) and thresholded (y-axis) synthetic noise stimuli. The dashed black line represents a 1:1 relationship between the two image types, and the red line depicts the measured relationship. For shallow slopes (i.e. 0.25) there is almost a 1:1 relationship between the measured slopes of grayscale and thresholded stimuli. However, as shown in Fig. 3A, from shallow 1/f slope conditions (i.e. 0.25) to steeper 1/f slope conditions (i.e. 2.25), the 1/f slope for thresholded images becomes shallower compared to their grayscale counterparts as a consequence of the thresholding procedure.

they were derived. Thresholded images result in a shallower 1/f slope, particularly at steeper 1/f slope values (i.e. 1.75 and 2.25) (Fig. 3).

While the photometric properties between grayscale and thresholded image types differ, their geometric properties (structure) are relatively similar. In particular they are similar in their fractal-like scaling characteristics. Fractal dimension (*D*) is a scaling parameter that quantifies the shape of the boundary contours between image regions of different intensity (in the case of a thresholded image this is

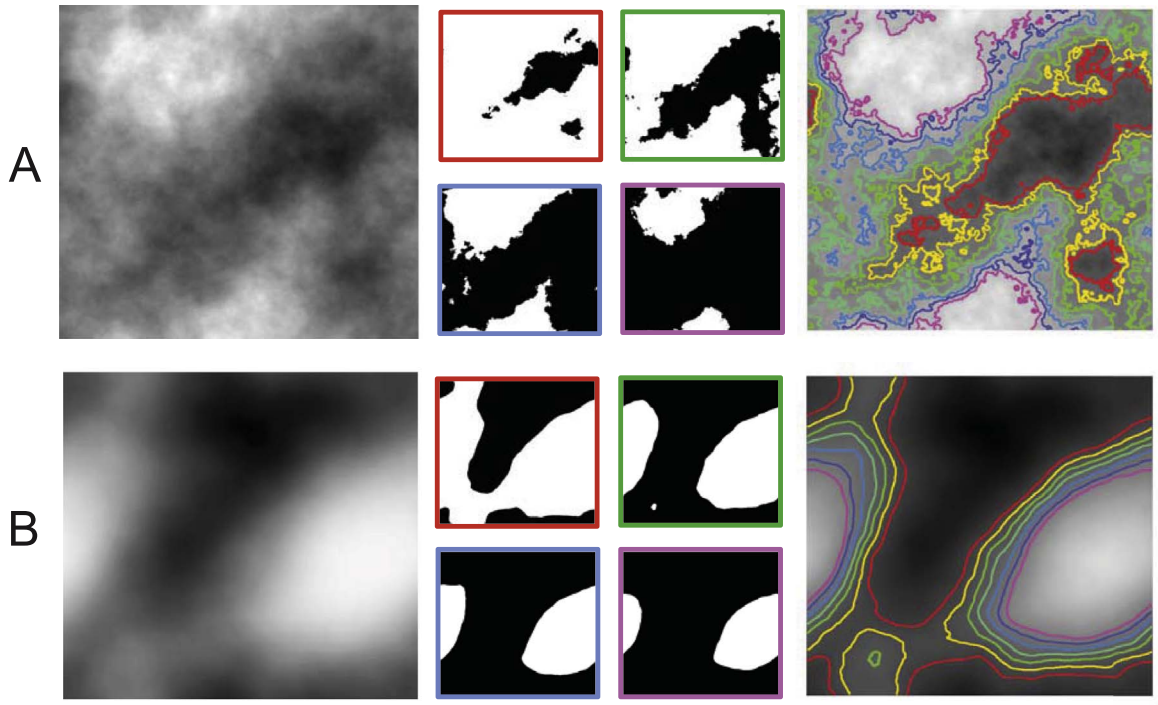

Fig. 4. Fractal analysis of grayscale synthetic noise images at different threshold levels as illustrated in Spehar and Taylor (2013).The grayscale synthetic noise images on the leftmost panels have 1/f slopes of 1.5 (A) and 2.0 (B). The four smaller segments in the middle are thresholded black and white versions of the grayscale image at different luminance levels: at 20% (red) 40% (green), 60% (blue) and 80% (purple). The extracted contours in these images have the same fractal characteristics, which is depicted in the rightmost image in both A and B, where the extracted contours from thresholded images are superimposed on the original grayscale image. The average fractal dimension D of these contours equals 1.425 (ranging from 1.39 to 1.44) in A and 1.082 (ranging from 1.075 to 1.090) in B.

the boundary contour between the paint-filled and empty regions) (Mandelbrot, 1982; Spehar et al., 2003). Although grayscale synthetic noise images have continuous intensity variations, and, as such, do not contain explicitly visible contours, one can think of them as being composed of a series of superimposed, or nested, contours each existing at a particular intensity level. To confirm these assertions, Spehar and Taylor (2013) performed the analysis illustrated in Fig. 4. They thresholded grayscale synthetic noise images at a number of different intensity levels below and above mean luminance. Fig. 4 illustrates thresholding at 20%, 40% (mean luminance), 60%, and 80% for grayscale synthetic noise images with 1/f slopes of 1.5 (Fig. 4A) and 2.0 (Fig. 4B) respectively.

In both Fig. 4A and B, the leftmost panel represents the original grayscale image and the rightmost panel depicts a series of contours, each of constant grayness, corresponding to different threshold values (20%–80%). The four middle panels show examples of such thresholded images at levels of 20%, 40%, 60% and 80%. Although grayscale synthetic noise images do not contain sharp luminance boundaries, this analysis shows that each of the grayscale images can be pictured as a series of nested contour patterns at different threshold intensities. It is evident from the superimposed contour graph depicted on the right in Fig. 4 that, within a given grayscale pattern, the fractal characteristics of all the contours appear to be identical. This can be verified empirically by performing a box counting analysis on each set of contours (Spehar and Taylor, 2013). For each of the images, the box-count fractal dimensions for a set of nested constituent contours corresponding to a given grayscale image were the same within measurement uncertainty. This was also the case in the set of stimuli used in the present study, whereby our grayscale and thresholded stimuli had the same fractal dimension despite having different measured 1/f slope values (Table 1).

2.5. Procedure

2.5.1. Retinotopic mapping

Retinotopic mapping procedures were conducted in order to identify visual areas V1, V2, and V3. These procedures are described in more detail in previous work (Schira et al., 2009, 2007). Retinotopic mapping was either recorded in the same MRI session as Experiment 1 or 2, or for some subjects in separate MRI sessions. All subjects were presented cyclic stimuli that consisted of rotating wedges, providing phase encoded polar angle maps. Visual areas V1, V2, and V3 were defined from our polar angle retinotopic mapping procedure, which allowed for a region of interest (ROI) analysis on the voxels within each visual area.

Across both experiments, most subjects (n=16/21) also participated in an eccentricity mapping paradigm (expanding rings) in order to enable the analysis of responses at different eccentricity ranges. For the subjects that did not undergo eccentricity mapping (n=5), an anatomical template of retinotopy (Benson et al., 2014; Benson et al., 2012) was fitted using Freesurfer (v5.3) (http://surfer.nmr.mgh.harvard.edu/) (Fischl and Dale, 2000; Fischl et al., 1999; Salat et al., 2004) in order to approximate the cortical location of the eccentricity ranges found in our own mapping procedures. A fixed range of eccentricities were obtained in our own mapping procedures, and as such the same range of eccentricities were derived via the Benson template. These ranges included, from the fovea to the periphery, 0.00°–0.48°, 0.48°–0.95°, 0.95°–1.36°, 1.36°–1.93°, 1.93°–2.74°, 2.74°–3.89°, 3.89°–5.50°. Therefore, 7 ROIs were created for each eccentricity range within V1, V2, and V3.

2.5.2. Filtered noise experiments

Experiment 1 and 2 were conducted in a block design manner with an initial 12 s of fixation on a mean luminance gray screen (Fig. 1B). Each block consisted of 5 synthetic noise images that were each presented for 1 s with an inter-stimulus interval (ISI) of 200 ms, resulting in a total block time of 6 s. Each stimulus was faded in and

out using a cosine ramp function with a rise time of 500 ms at full contrast and then fading out over 500ms. During the ISI, a blank gray screen at mean luminance was presented.

The images within each block all had the same 1/f slope and the same contrast level (10% or 30%) (Exp 1) or image type (grayscale or thresholded) (Exp 2). Images with differing 1/f slope values, contrast levels (Exp 1), and image types (Exp 2) were not intermixed within a block in order to allow the analysis of 1/f slope, contrast (Exp 1), and image type (Exp 2) effects individually. This design resembles a typical block design (as in Grill-Spector et al., 1999; Kanwisher et al., 1997; Schira and Spehar, 2011) but with relatively short blocks to avoid fatigue and to make a single aesthetic judgment over an entire block feasible.

Each block of images was followed by a 3 s period for responses and then 7 s of fixation to allow BOLD response levels to return to baseline. Blocks were grouped into runs (periods of continuous fMRI scanning) each consisting of 20 blocks lasting ~332 s, and each run was repeated between 3–5 times for each task condition. For Experiment 1, in a run each 1/f slope condition was repeated four times in a randomized sequence: twice at 10% contrast and twice at 30% contrast. Experiment 2 had the same design, except each 1/f slope condition was repeated twice for the grayscale image type, and twice for the thresholded image type.

Two tasks were employed in both Experiment 1 and 2 in order to manipulate attention. The first task was an Aesthetic Rating (AR) task, where subjects had to indicate their overall preference of each block of images on a scale of 1 to 4 on a Likert scale (Strongly Dislike, Somewhat Dislike, Somewhat Like, and Strongly Like) via button press.

The second task consisted of a Central Visual Search (CVS) paradigm, which was a modified version of Braun's (1994) letter task. For this, T and L letter combinations were overlaid on top of synthetic noise images. Two combinations of letters were used: 1) 1 T 4 L's and 2) 5 L's. The letters were presented at 5 different positions: at the center and around the center at 0°, 90°, 180°, or 270° (Fig. 1B). To increase task difficultly each letter was randomly rotated by either 45°, 135°, 225°, and 315°. Furthermore, the letter L was randomly flipped horizontally when present. To make the visibility of the search set equalized across experimental images with varying 1/f slopes, a gray disk at mean luminance was present behind the letters (Fig. 1B). The letter and disk overlays were created using Adobe Illustrator CS6 (Version 16.0). Over each of the 5 noise images within a block, 5 different letter configurations were overlaid at random. For each configuration, no more than one T was present (1 T 4 L's), and in some configurations the target letter T was absent (5 L's) Subjects were instructed to search and count the total number of times the letter T was presented within each block, which could vary in frequency from 1 to 4. At the end of each block, subjects were instructed to count and report via button press how many times the target letter (T) was present.

The two task conditions were not intermixed within a run and subjects were instructed verbally and visually to as to which task they had to perform at the beginning of each run, either Aesthetic Rating (AR) or Central Visual Search (CVS). Subjects were also instructed within each run via a 3 s instruction screen after each block which stated “Preference Rating” (AR) or “How many target letters were present?” (CVS) depending on the task for the run. Subjects responded using 2 Lumina response pads (Cedrus Corporation, San Pedro, CA) that were placed in each hand. Each response pad had 2 buttons that corresponded to the 4 options presented on the screen.

2.6. Data acquisition

Data was acquired with a Philips 3 T Achieva X Series equipped with Quasar Dual gradients and a 32-channel head coil. For polar angle mapping and both filtered noise experiments, functional EPI images were acquired in 32 axial slices covering the whole head, with 180 (retinotopic mapping) and 167 (filtered noise experiments) volumes respectively. The voxel resolution of these images was 2×2×2.5 mm, resulting from 2.5 mm slice thickness, a 96×96 matrix (ascending acquisition), and a field of view (FOV) of 192 mm. Images were acquired with a repetition time (TR) of 2 s, an echo time (TE) of 25 ms, and an acceleration (SENSE) factor of 3. For 6 of the 21 subjects across both experiments, eccentricity mapping was conducted in a separate session. Also, for some subjects, retinotopic mapping was recorded at a higher resolution more optimal for retinotopic mapping purposes. For this, EPI images were acquired at a higher resolution, but only covering the occipital pole. The voxel resolution of these images were 1.5×1.5×1.5 mm, 32 oblique coronal slices, a 128×128 matrix (ascending acquisition), and a FOV of 192 mm. These images were acquired with a TR of 2 s, a TE of 25 ms and a SENSE factor of 2. For cortical surface reconstructions, high-resolution structural scans were acquired for each subject using a magnetization-prepared rapid acquisition with gradient echo (MPRAGE) protocol with a resolution of 0.75×0.75×0.75 mm.

2.7. Data analysis

2.7.1. Aesthetic rating and central visual search task performance

Task performance was analyzed in order to ensure that each participant was performing the task as required. In addition, a repeated measures ANOVA was conducted on the aesthetic ratings in order to test for main effects and interactions of 1/f slope, contrast (Exp 1), and image type (Exp 2) conditions. A repeated measures ANOVA was also conducted on the accuracy scores of the CVS task to assess if performance was comparable across all 1/f slope, contrast (Exp 1), and image type (Exp 2) conditions.

2.7.2. fMRI data

Images acquired from the scanner were pre-processed before analysis. This included slice scan time correction as well as motion correction, which were both conducted using SPM8 (SPM software package, Wellcome Department, London, UK; http://www.fil.ion.ucl.ac.uk/spm/) and custom lab scripts.

For retinotopic mapping, traveling-wave analysis procedures were conducted using the mrVista Toolbox (Stanford University, Stanford, CA; http://white.stanford.edu/software/) with correlational analysis. The cyclic retinotopic mapping data was analyzed using a fast Fourier transform (FFT) based correlation analysis, as built in the mrLoadRet software from the mrVISTA toolbox. This estimates a coherency value for each voxel in cortex as a ratio between power at stimulus frequency and noise. The retinotopic location for each voxel is determined by the phase value at the stimulus frequency. This can then be displayed on a 3D rendered brain surface using a color map that has a color assigned for each phase. Polar angle maps generated from this analysis allowed for visual areas V1, V2, and V3 to be defined as regions of interest (ROI).

Further analysis in the mrVista Toolbox included a general linear model (GLM) of responses across visual areas (V1, V2, and V3) and a range of eccentricities within these areas (0.00°–0.48°, 0.48°–0.95°, 0.95°–1.36°, 1.36°–1.93°, 1.93°–2.74°, 2.74°–3.89°, 3.89°–5.50°). A GLM models the relationship between the experimental manipulations and the observed BOLD response assuming both the experimental paradigm and hemodynamic response function (HRF) are known (Lindquist, 2008). The experimental paradigm indicates each stimulus condition onset, while a canonical HRF is used to model the typical response profile of the BOLD response. In the present study, the Boynton Gamma HRF was used (Boynton et al., 1996). After β weights were calculated, a repeated measures ANOVA was performed on these values in order to determine the effects of each condition individually across visual areas and a range of eccentricities within each visual area.

3. Results

We measured the BOLD response in early visual cortex (V1, V2, and V3) to synthetic noise images that varied in their 1/f slope (0.25, 0.75, 1.25, 1.75, 2.25) at different contrast levels (10% and 30%) in Experiment 1. To investigate to what extent the BOLD response is driven by the photometric (intensity-based) properties of our stimuli, in Experiment 2 we measured the BOLD response to the same range of 1/f slopes as Experiment 1 but across two different image types: 1) grayscale, containing both photometric and geometric image properties and 2) their thresholded counterparts containing only geometric characteristics. In both experiments responses were measured under two task conditions that modulated attention: 1) Aesthetic Rating (AR), where subjects were actively rating their preference toward each block of images, and 2) a Central Visual Search (CVS) task during which subjects passively viewed images while their attention was captured by a visual search task at the center of each stimulus.

3.1. Behavioral results: central visual search task and aesthetic ratings

For the AR task, we conducted a two-way, repeated measures ANOVA on preference ratings with the factors contrast (10% and 30%) and 1/f slope (0.25, 0.75, 1.25, 1.75, 2.25) for Experiment 1, and the factors image type (grayscale and thresholded) and 1/f slope (0.25, 0.75, 1.25, 1.75, 2.25) for Experiment 2. 1/f slope did not reach significance in Experiment 1 ($F_{1.265,12.653}$=.599, p=0.491), but was significant for Experiment 2 ($F_{2.323,20.907}$=4.349, p=0.022). No other main effects or interactions reached significance.

Preference ratings across each 1/f slope condition followed the same trend in both experiments, whereby preference ratings increased from 1/f slope conditions 0.25 to 0.75 and then leveled off between 1.25 and 2.25 for all image types (Fig. 5A and B). These findings are consistent with previous reports that aesthetic preference is higher for images (natural or synthetic) that follow the statistical properties of natural scenes (Juricevic et al., 2010; Spehar and Taylor, 2013; Spehar et al., 2015).

In the CVS task, participants were on average 70.03% (SD=21.66) correct in Experiment 1 and 76.67% (SD=23.81) correct in Experiment 2. We conducted a two-way repeated measures ANOVA on performance accuracy across the factors contrast (10% and 30%) and 1/f slope (0.25, 0.75, 1.25, 1.75, 2.25) for Experiment 1, and image type (grayscale and thresholded) and 1/f slope (0.25, 0.75, 1.25, 1.75, 2.25) for Experiment 2 to analyze accuracy across conditions. The factor of 1/f slope reached significance in Experiment 1 ($F_{3.049,30.493}$=3.027, p=0.044), but not in Experiment 2 ($F_{2.363,21.269}$=1.355, p=.282). No other main effects or interactions reached significance.

In Experiment 1 there was approximately a 10% drop in accuracy for the natural 1/f slope condition (1.25) (Fig. 5C). Although somewhat unexpected, this drop off is consistent with previously reported surround contrast suppression in natural images (McDonald and Tadmor, 2006). When a central object is surrounded by an image with a natural $1/f^{\alpha}$ amplitude spectrum, the perceived contrast of the central object is decreased (McDonald and Tadmor, 2006), which may have been detrimental to CVS task performance. However, the same pattern of responses was not found in Experiment 2 (Fig. 5D), suggesting that this is not a very robust effect.

3.2. Overall visual cortex analysis

Across both experiments, a GLM analysis was conducted to model the contribution of each condition to the magnitude of the BOLD response in visual areas V1, V2, and V3. A four-way repeated measures ANOVA was conducted on the β weights calculated from the aforementioned GLM analysis. For Experiment 1, the four within subject factors included visual area (V1, V2, V3), task (AR, CVS), contrast (10% and 30%) and 1/f slope (0.25, 0.75, 1.25, 1.75, and 2.25). For Experiment 2, the four within subject factors included visual area (V1, V2, V3), task (AR, CVS), image type (grayscale and thresholded), and 1/f slope (0.25, 0.75, 1.25, 1.75, and 2.25).

The β weights calculated in the GLM analysis for both experiments are summarized in Tables 3 (Exp 1) and 4 (Exp 2) of the Supplementary Materials. Also, all main effects and interactions output from the ANOVA of both experiments are summarized in Tables 5 and 6 of the Supplementary Materials, and those of relevance will be individually presented in text below. Finally, pairwise comparisons of

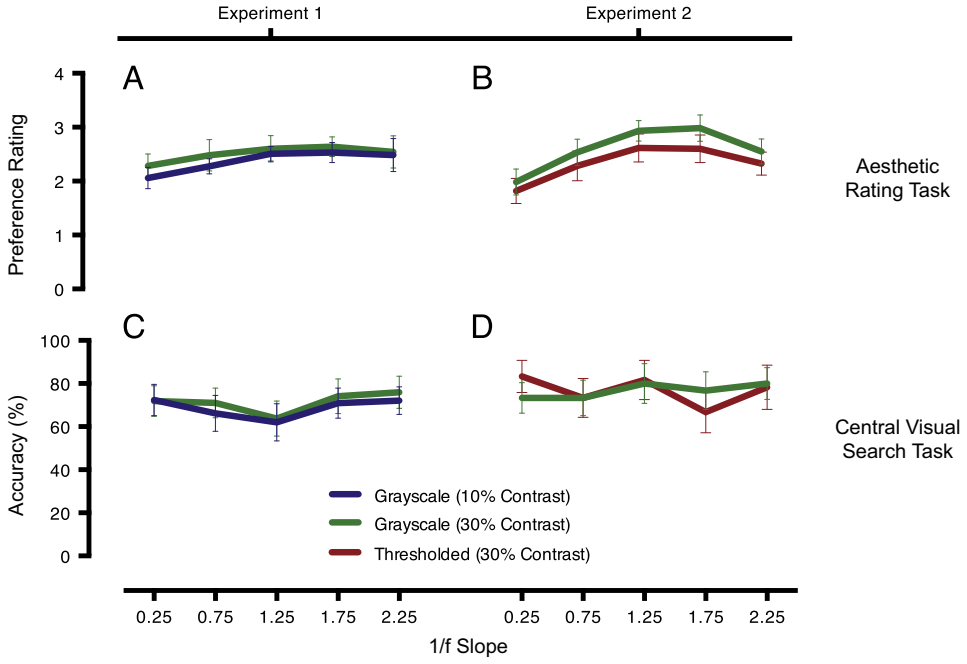

Fig. 5. Behavioral results for both Aesthetic Rating (AR) and Central Visual Search (CVS) tasks. Averaged preference ratings for the AR task (A & B) and averaged accuracy for the CVS task (C & D) are depicted for each contrast level (10% and 30%) (Exp 1) and image type (grayscale and thresholded) (Exp 2) across each 1/f slope condition (0.25, 0.75, 1.25, 1.75, 2.25). Error bars depict SEM between subjects.

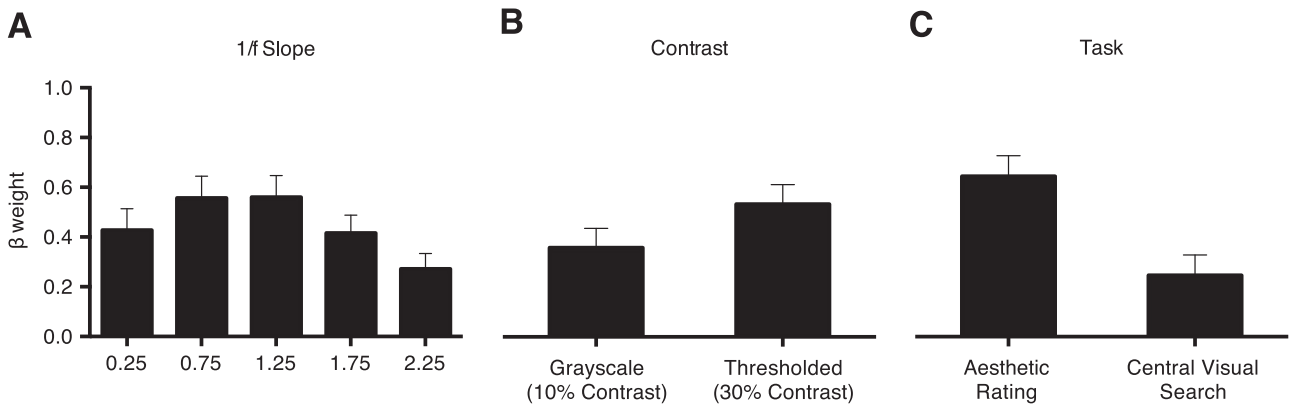

Fig. 6. Estimated marginal means of β weights in Experiment 1 for each 1/f slope (A), contrast (B), and task (C) condition. Marginal means were calculated by collapsing the β weights of each factor across all other factors, whereby (A) is an average across visual area, contrast, and task conditions, (B) is an average across visual area, 1/f slope, and task conditions, and (C) is an average across visual area, 1/f slope, and contrast conditions. Note that both 1/f slope and task conditions have larger effects on the BOLD amplitude than contrast. Error bars depict SEM between subjects.

each 1/f slope condition are presented in Tables 7 (Exp 1) and 8 (Exp 2) of the Supplementary Materials.

3.2.1. Experiment 1: 1/f slope and contrast manipulation

In agreement with our initial hypothesis, there was a significant main effect of 1/f slope ($F_{1.696,16.959}$=29.349, p=0.000), whereby responses on average resembled an inverted U-shape peaking at a natural 1/f slope of 1.25 (Fig. 6A). This pattern of responses was also present in across most visual areas, task, and contrast conditions (Fig. 7). When response curves did not peak at 1.25, they peaked at 0.75, which is closely within the range of 1/f slopes present in nature (0.8 to 1.5, mean=1.2) (Tolhurst et al., 1992). The difference in peak responses observed across visual areas, task, and contrast conditions is discussed further in Section 3.2.3 in relation to the 1/f slope and visual area interaction. The inverted U-shaped response profile peaking at either 0.75 and 1.25 suggests that early visual cortex is tuned to natural 1/f spectra, which may possibly be explained by the theory of response equalization rather than sparse coding (Brady and Field, 1995; Field, 1987; Field and Brady, 1997).

Response equalization predicts that the neuronal response magnitude in visual cortex increases in proportion to SF. In the presence of an image that has a natural 1/f slope, this model predicts a flat response across all SFs, which would suggest that cellular responses and properties in early visual cortex are optimized to most efficiently process the statistical properties of natural scenes such as the $1/f^{\alpha}$ amplitude spectrum. This would allow information across different spatial scales to be represented by neurons with a similar dynamic range that is present in the natural environment (Field and Brady, 1997).

There was also a significant main effect of contrast ($F_{1,10}$=100.746, p=0.000), indicating that across all visual areas (V1, V2, and V3) the higher contrast condition (30% grayscale) resulted in larger BOLD responses compared to the lower contrast condition (10%) across all task and 1/f slope conditions (Fig. 6B and Fig. 7). This can be attributed to the contrast response function, which is well established in early visual cortex (Boynton et al., 1996; Buracas and Boynton, 2007; Xing et al., 2013), and has also been reported in experiments more similar to the present study (Olman et al., 2004; Rieger et al., 2013). There was also a significant visual area by contrast interaction ($F_{1.471,14.705}$=15.693, p=0.001) showing that although stimuli with higher contrast elicit a higher BOLD response across all 3 visual areas (Fig. 7), there are clear differences in each area's degree of contrast dependence. Consistent with previous work (Boynton et al., 1996; Buracas and Boynton, 2007; Tong et al., 2012; Tootell, 1995), the largest difference in response magnitude between low (10%) and high (30%) contrast stimuli is observed in V1, while in V2 and V3 this

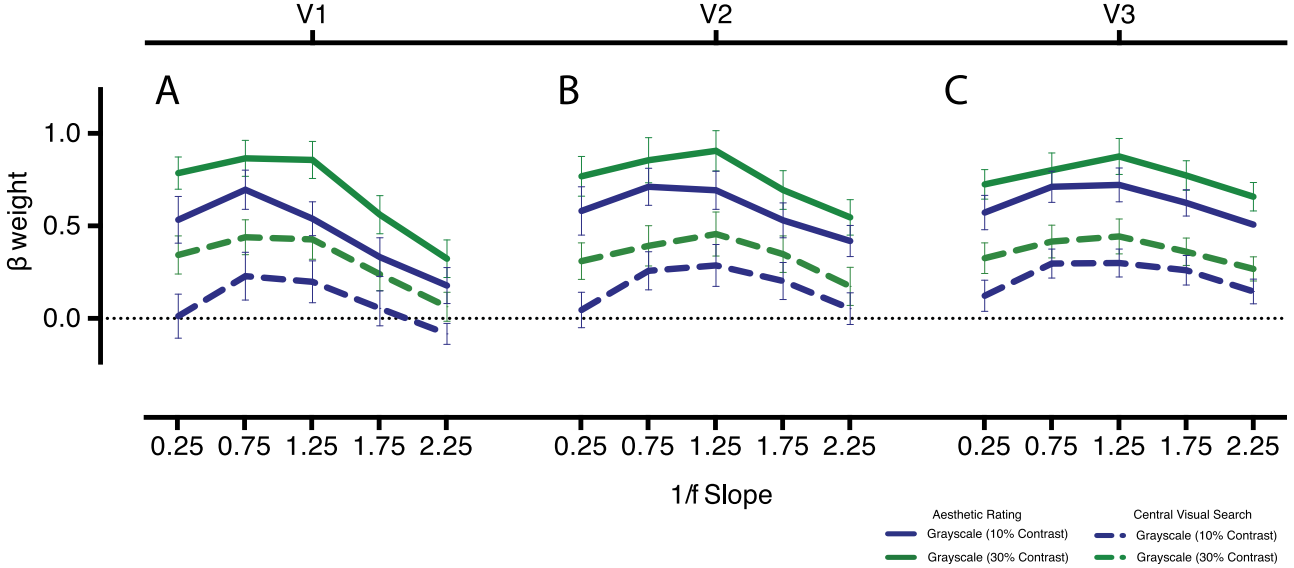

Fig. 7. GLM β weights averaged across subjects for V1 (A), V2 (B), and V3 (C) for Experiment 1. β weights are depicted for each task (AR, CVS) and contrast (10% and 30%) condition as a function of 1/f slope (0.25, 0.75, 1.25, 1.75, and 2.25). Error bars depict SEM between subjects.

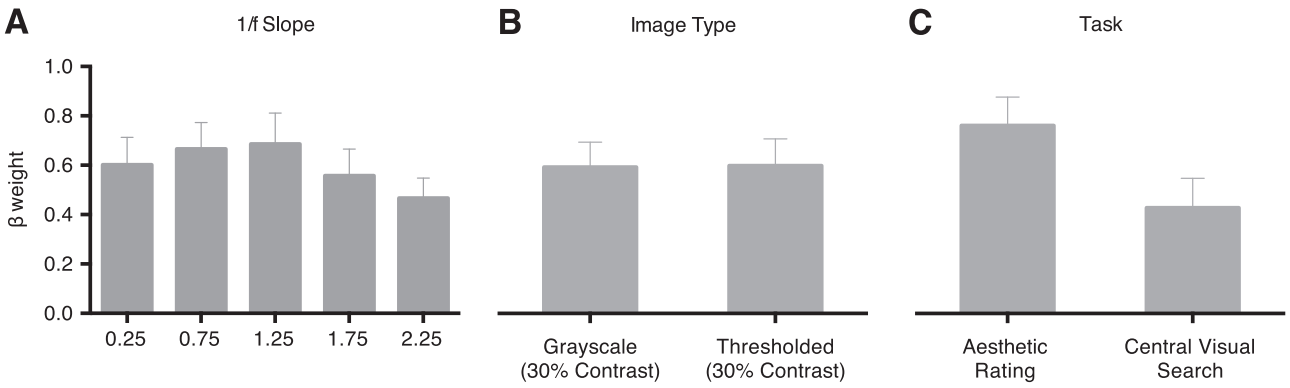

Fig. 8. Estimated marginal means of β weights for each 1/f slope, image type and task condition. Marginal means were calculated by collapsing the β weights of each factor across all other factors, whereby (A) is an average across visual area, image type, and task conditions, (B) is an average across visual area, 1/f slope, and task conditions, and (C) is an average across visual area, 1/f slope, and image type conditions. Error bars depict SEM between subjects.

difference is comparatively lower (Fig. 7).

3.2.2. Experiment 2: Grayscale vs. Thresholded image manipulation

Following the findings of Experiment 1, we investigated whether the BOLD response is driven by the photometric (intensity based) properties of our stimuli or by their geometric (fractal) properties. Firstly, we replicated the findings of Experiment 1 whereby the effect of 1/f slope was significant and the pattern of responses on average reflected an inverted U-shape peaking for 1.25 (Fig. 8A). As in Experiment 1, we found that the peak response across visual areas for each task and image type condition ranged between 0.75 and 1.25, which is within the range 1/f slopes found in nature. Surprisingly, responses tended to be high for thresholded stimuli with an input 1/f slope of 2.25 in the CVS task condition (Fig. 9). Since the measured 1/f slope of thresholded images with an input slope of 2.25 is 1.55 (Table 1), one may predict high BOLD responses since its measured 1/f slope is close to the range present in nature. However, we attribute the larger responses observed to noise as responses to thresholded images with an input 1/f slope of 1.75 have comparatively lower responses (Fig. 9). The measured 1/f slope of thresholded images with an input slope of 1.75 is 1.36, which is close to a slope of 1.25 and as such should elicit similar responses.

The main effect of image type was non significant ($F_{1,9}$=0.151, p=0.707), and did not have any significant interactions with other factors such as 1/f slope ($F_{2.470,22.231}$=1.308, p=0.294). The two image types in this experiment had the same contrast level (30%, *SD*=0.000) and mean luminance (127.5, *SD*=38.239), however they varied in their image characteristics, either being grayscale (containing both geometric and photometric characteristics) or thresholded (containing only geometric characteristics). Since these two image types have a different distribution of luminance intensities (see Table 1 and 2 of the Supplementary Materials) and consequently different measured 1/f slopes (Table 1), one could expect differential activity in early visual cortex between grayscale and thresholded stimuli. However, there is no significant difference in the BOLD response elicited across the two different image types (Fig. 8B). This is also apparent in each visual area (V1, V2, and V3), depicted in Fig. 9, where overlapping response profiles are observed across 1/f slope conditions for both grayscale and thresholded image types. This suggests that the BOLD response is predominantly driven by the structural (geometric) characteristics of both grayscale and thresholded stimuli despite differences in their visual appearance, $1/f^{\alpha}$ amplitude spectra, and photometric characteristics (luminance distributions).

3.2.3. Effects and interactions across both experiments

Across both experiments there was a significant main effect of task (Exp 1: $F_{1,10}$=50.250, p=0.000; Exp 2: $F_{1,9}$=9.886, p=0.012), whereby responses were higher when subjects were attending to the synthetic noise images during the AR task compared to the CVS task where subjects passively attended (Exp 1: Fig. 6C and 7, Exp 2: Figs. 8C and 9). This is consistent with the established effects of attention in modulating the BOLD response in early visual cortex (Brefczynski

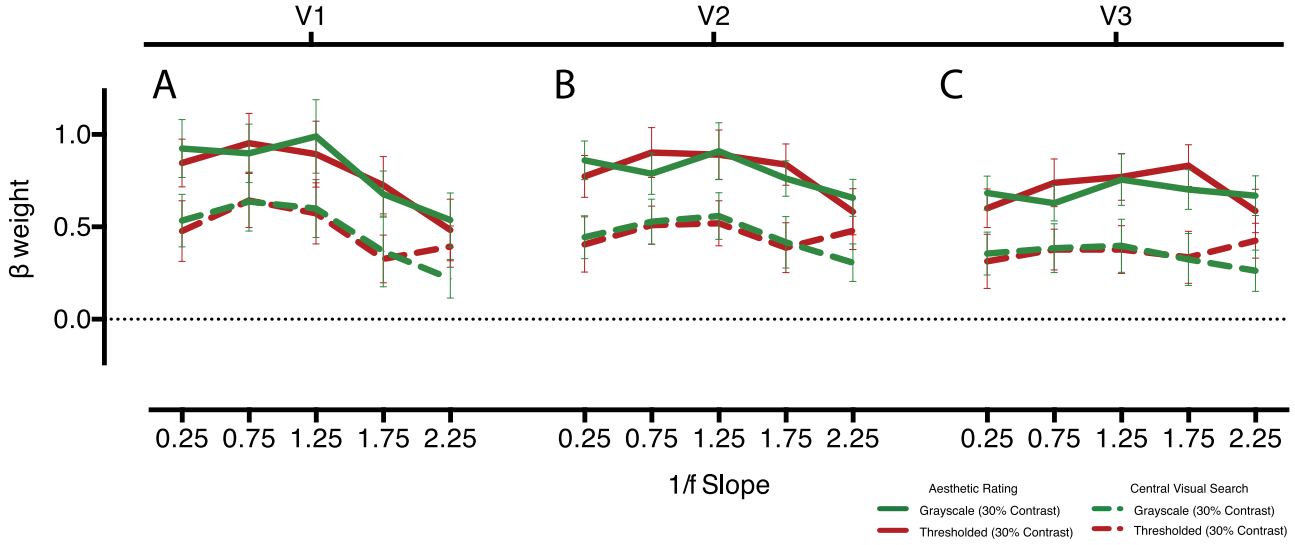

Fig. 9. GLM β weights averaged across subjects for V1 (A), V2 (B), and V3 (C) for Experiment 2. β weights are depicted for each task (AR, CVS) and image type (grayscale and thresholded) as a function of 1/f slope (0.25, 0.75, 1.25, 1.75, and 2.25). Error bars depict SEM between subjects.

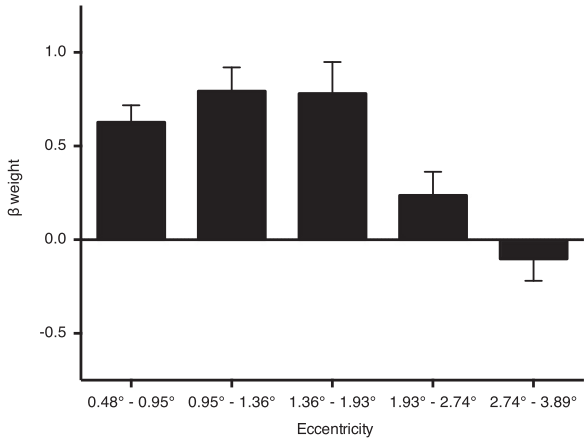

Fig. 10. Estimated marginal means of β weights for each eccentricity range averaged across visual areas V1, V2, and V3 for Experiment 1. Marginal means were calculated by collapsing the β weights of each factor across all other factors, where the data in this plot is an average across all visual area, task, contrast, and 1/f slope conditions. Error bars depict SEM between subjects.

and DeYoe, 1999; Chawla et al., 1999; Tootell et al., 1998). Therefore, the effect of task can be attributed to the attention boost gained when "actively" rating each stimulus compared to "passively" viewing stimuli in the background while attending to CVS task.

There was no significant main effect of visual area in either experiment (Exp 1: $F_{1.525,15.248}$=2.559, p=0.120; Exp 2: $F_{1.177,10.590}$=1.604, p=0.237). However, there was a significant visual area by 1/f slope interaction (Exp 1: $F_{2.787,27.868}$=30.941, p=0.001; Exp 2: $F_{3.206,28.857}$=28.297, p=0.000), whereby the response profile in V1 across all contrast (Exp 1), image type (Exp 2) and task conditions is asymmetric compared to V2 and V3 with responses saturated between 1/f slopes 0.25 to 1.25 (Exp 1: Fig. 7A, Exp 2: Fig. 9A). Also, when collapsing across all experimental manipulations responses in V1 peak at 0.75 whereas V2 and V3 peak at 1.25 (see Fig. 1 of Supplementary Materials). This is also the case across most task, contrast (Exp 1) and image type (Exp 2) conditions (Figs. 7 and 9). This finding is consistent with previous investigations into the SF tuning properties of early visual areas, which have measured the BOLD response to isolated SFs (Henriksson et al., 2008; Singh et al., 2000; Tong et al., 2012). They have found V1 to have narrower tuning for high SFs compared to V2 and V3, which are more broadband tuned in comparison. Since shallower 1/f slopes such as 0.25 and 0.75 contain more power in the high SF domain than steeper 1/f slopes (Fig. 1A), the SF tuning properties of V1 are consistent with the saturated responses elicited for shallower 1/f slopes (0.25 and 0.75).

There was also a significant three-way interaction between visual area, task, and 1/f slope in Experiment 1 ($F_{3.750,37.502}$=4.449, p=0.006). This interaction was not significant for Experiment 2, but the trend was present ($F_{3.191,28.720}$=2.531, p=0.074). Specifically, the magnitude of response modulation by task condition (AR vs. CVS) increases from V1 to higher visual areas (V2 and V3), and this effect was larger for the steeper 1/f slope conditions (1.75 and 2.25; see Fig. 7). This is consistent with the well-documented effects of attention in the literature, showing V1 to be less sensitive to the effects of attention compared to later visual areas V2 and V3 (Bressler et al., 2013; Kastner et al., 1999; Liu et al., 2005; Tong et al., 2012; Tootell et al., 1998). The reason the effect of task may be stronger for steeper 1/f slopes may be attributed to the spatial tuning properties of V1, V2, and V3.

3.3. Eccentricity analysis

It has been established in previous work (Daniel and Whitteridge, 1961; De Valois et al., 1982; Henriksson et al., 2008; Sasaki et al., 2001; Talbot and Marshall, 1941) that high SF channels are predominantly located in the fovea, compared to the periphery which predominately has low SF channels. Due to this, we investigated how the tuning of early visual cortex toward the $1/f^{\alpha}$ amplitude spectrum is modulated as a function of eccentricity. Consequently, we conducted a GLM analysis to model the contribution of each condition to the magnitude of the BOLD response across individual eccentricity bands ranging from the fovea toward the periphery.

For Experiment 1, we conducted an ANOVA on the β weights calculated from this GLM analysis across the factors visual area (V1, V2, V3), eccentricity (0.48°–0.95°, 0.95°–1.36°, 1.36°–1.93°, 1.93°–2.74°, 2.74°–3.89°), task (AR and CVS), contrast (10% and 30%) and 1/f slope (0.25, 0.75, 1.25, 1.75, and 2.25) as within-subject factors. For Experiment 2, we conducted an ANOVA across the factors visual area (V1, V2, V3), eccentricity (0.48°–0.95°, 0.95°–1.36°, 1.36°–1.93°, 1.93°–2.74°, 2.74°–3.89°), task (AR and CVS), image type (grayscale and thresholded) and 1/f slope (0.25, 0.75, 1.25, 1.75, and 2.25) as within-subject factors. The β weights calculated in this GLM analysis are summarized in the Supplementary Materials and can be found in Tables 9 (V1), 10 (V2), and 11 (V3) for Experiment 1 and Tables 12 (V1), 13 (V2), 14 (V3) for Experiment 2. All main effects and interactions from Experiments 1 and 2 are summarized in Tables 15 and 16 of the Supplementary Materials respectively.

For some subjects not all eccentricity ranges could be determined due to eccentricity maps of insufficient quality and were hence excluded from the Eccentricity Analysis (Exp 1: N=3/11, Exp 2: N=1/10). Also, the most foveal (0.00°–0.48°) and peripheral (3.89°–5.10°) eccentricity ranges were not included in the ANOVA in order to discount the effects of the central disk present in the CVS task (0.00° to 0.50° from center gaze) and the mean luminance gray background (3.89°–5.10°). These ranges, however, are plotted in Fig. 11 (Exp 1) and Fig. 13 (Exp 2) in order to depict how effective the Central Visual Search task was in the central 0.5 degrees (Figs. 11 and 13) and to show how responses drop off in the most peripheral eccentricity range (3.89° to 5.50°) where the stimulus was not present.

All the factors in the Eccentricity Analysis that overlap with the Overall Visual Cortex Analysis across both Experiment 1 and 2 follow the same trend whereby the main effects of 1/f slope (Exp 1: $F_{1.435,10.047}$=17.155, p=0.001; Exp 2: $F_{2.548,20.382}$=7.549, p=0.002), contrast (Exp 1: $F_{1,7}$=79.486, p=0.000), and task (Exp 1: $F_{1,7}$=47.060, p=0.000; Exp 2: $F_{1,8}$=13.647, p=0.006) reach significance, while visual area (Exp 1: $F_{1.920,13.438}$=.230, p=0.789; Exp 2: $F_{1.325,10.599}$=2.440, p=0.144) and image type (Exp 2: $F_{1,8}$=0.198, p=0.668) do not. The direction of responses across all the aforementioned factors is also consistent with the Overall Visual Cortex Analysis. For this reason, only the main effect of eccentricity will be presented in text below as well as interactions involving this main effect.

3.3.1. Experiment 1: 1/f slope and contrast manipulation

The main effect of eccentricity was significant ($F_{1.632,11.422}$=15.575, p=0.001) and the direction of this effect shows that the BOLD response is highest for eccentricity ranges 0.95°–1.36° and 1.36°–1.93° and is lowest for the most peripheral eccentricity ranges 1.93°–2.74° and 2.74°–3.89° (Fig. 10). These results show that the BOLD response is modulated as a function of eccentricity, which is consistent with previous research investigating attentional modulation of the BOLD response across eccentricity ranges (Bressler et al., 2013). If a task requires subjects to fixate and attend to the center of the display, the BOLD response across visual areas V1, V2, and V3 is modulated such that it is highest for foveal eccentricity ranges and decreases as eccentricity increases toward the periphery (Bressler et al., 2013).

There was also a significant eccentricity by contrast interaction ($F_{1.973,13.812}$=14.588, p=0.000). Across all visual areas (particularly V1) and task conditions, the difference in response magnitude between low (10%) and high (30%) contrast is largest for the most foveal

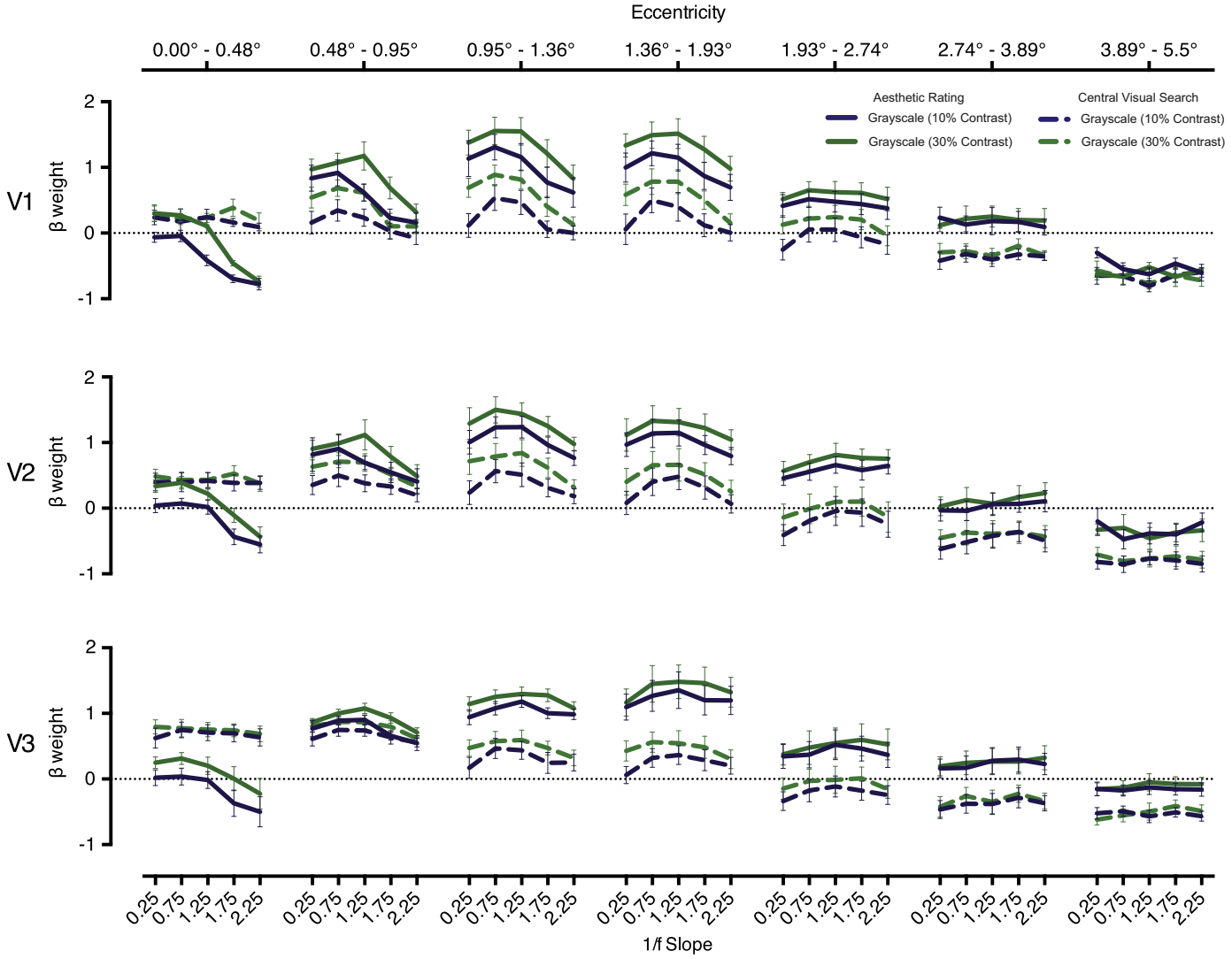

Fig. 11. GLM β weights for eccentricities ranging from the fovea toward the periphery (left to right) averaged across subjects for visual areas V1, V2, and V3 (top to bottom) for Experiment 1. β weights are depicted for each task (AR, CVS) and contrast (10% and 30%) condition as a function of 1/f slope (0.25, 0.75, 1.25, 1.75, and 2.25). Error bars depict SEM between subjects.

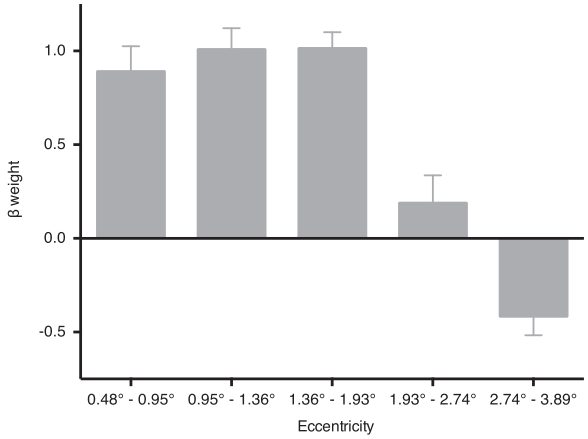

Fig. 12. Estimated marginal means of β weights for each eccentricity range averaged across visual areas V1, V2, and V3 for Experiment 2. Marginal means were calculated by collapsing the β weights of each factor across all other factors, where the data in this plot is an average across all visual area, task, image type, and 1/f slope conditions. Error bars depict SEM between subjects.

eccentricity range (0.48°–0.95°) and decreases systematically as eccentricity increases toward the most peripheral eccentricity range (2.74°–3.89°) (Fig. 11). This is consistent with previous research investigating contrast sensitivity as a function of eccentricity (Laron et al., 2009; Legge and Kersten, 1987; Xing et al., 2013) whereby responses saturate at higher contrast levels in the fovea compared to the periphery.

3.3.2. *Experiment 2: Grayscale vs. Thresholded image manipulation*

Replicating the findings of Experiment 1, the main effect of eccentricity was significant ($F_{1.602,12.819}$=42.003, p=0.000), whereby the pattern of responses show that foveal eccentricity ranges elicit higher BOLD activity compared to peripheral ranges (Fig. 12). Importantly, as in the Overall Visual Cortex Analysis, there was no significant effect of image type ($F_{1,8}$=0.198, p=0.668). This is apparent across all eccentricity bands whereby responses for both grayscale and thresholded image types overlap (Fig. 13). This suggests that even across individual eccentricity bands, the BOLD response is driven primarily by the geometric properties of our stimuli rather than their photometric properties. In terms of interactions, there was a significant interaction between eccentricity, task, and image type ($F_{2.837,22.699}$=5.464, p=0.006). This suggests that the pattern of responses are different for grayscale and thresholded image types across the two task conditions (AR and CVS) as a function of

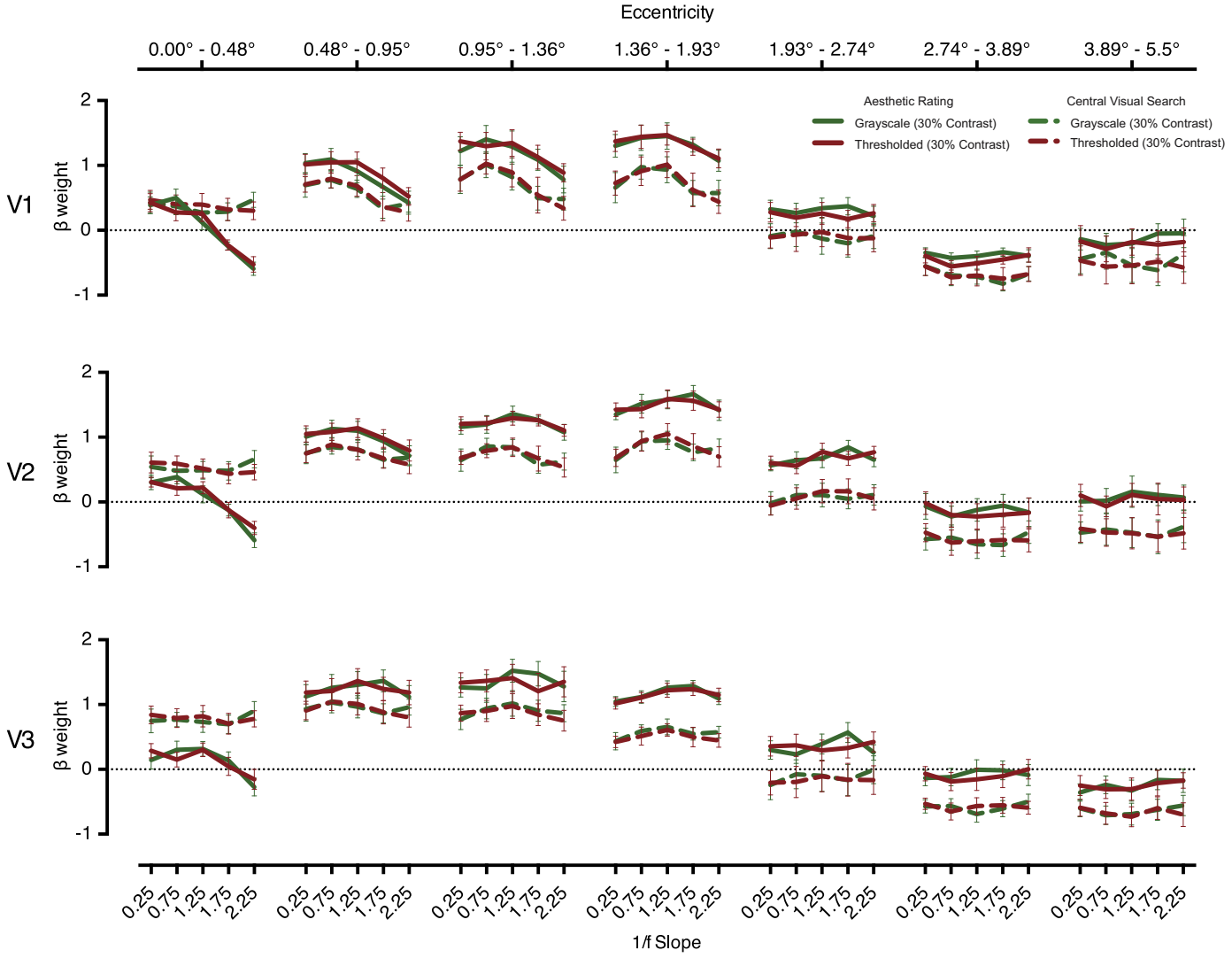

Fig. 13. GLM β weights for eccentricities ranging from the fovea toward the periphery (left to right) averaged across subjects for visual areas V1, V2, and V3 (top to bottom) for Experiment 2. β weights are depicted for each task (AR, CVS) and image type (grayscale and thresholded) condition as a function of 1/f slope (0.25, 0.75, 1.25, 1.75, and 2.25). Error bars depict SEM between subjects.

eccentricity, which was not part of our initial hypothesis. This may be due to nuanced differences in the shape (asymmetric vs. symmetric) of the response profile across the two experiments. However, the robustness and potential causes of these differences are yet to be determined.

3.3.3. Effects and interactions across both experiments

Between the two experiments there is some variability in which interactions were deemed significant ($p < 0.05$). Here, we only highlight interactions that were significant across both experiments.

Firstly, there was a significant interaction between eccentricity and 1/f slope (Exp 1: $F_{2.835,19.843}$=22.713 p=0.000; Exp 2: $F_{3.237,25.898}$=18.920, p=0.000) whereby the shape and peak of the BOLD response profile across 1/f slope conditions systematically changes from the most foveal eccentricity range (0.48°–0.95°) to the most peripheral (2.74°–3.89°) for all visual areas, contrast (Exp 1), image type (Exp 2), and task conditions. This is depicted in Fig. 14, whereby the most foveal eccentricity range (0.48°–0.95°) included in the ANOVA peaks at 0.75 and appears be asymmetric with saturated responses to 1/f slopes ranging from 0.75 and 1.25, whereas the parafoveal eccentricity range (1.36°–1.93°) appears to be more symmetric peaking at the natural 1/f slope of 1.25. The most peripheral eccentricity range (2.74°–3.89°) peaks at 1.75 and appears to be asymmetric with saturated responses to 1/f slopes ranging from 1.75 to 2.25. To see this interaction across experiments, task, contrast, and image type conditions individually see Fig. 11 (Exp 1) and 13 (Exp 2).

Fig. 14 plots responses that have been collapsed across both experiments and all manipulations, whereby most response profiles plotted (4/5) peak at a 1/f slope within the natural range of either 0.75 or 1.25 (Exp 1: Fig. 11, Exp 2: Fig. 13). Since shallow slopes (0.25) contain more power in the high SF domain and steeper slopes (2.25) contain more power in the low SF domain (Fig. 1A), this interplay between the preferred neural tuning toward a natural 1/f slope (1.25) and the eccentricity dependent distribution of SF selective neurons is reflected in the changes in response profile symmetry from the fovea (high SFs, fine spatial structure) and the periphery (low SFs, coarse spatial structure) (Daniel and Whitteridge, 1961; De Valois et al., 1982; Henriksson et al., 2008; Sasaki et al., 2001; Talbot and Marshall, 1941).

We also observe negative β weights across all visual areas, particularly for the most foveal eccentricity range as well as peripheral eccentricity ranges. Negative β weights correspond to negative BOLD responses (NBR), which can be considered as the level of suppression toward a stimulus. The more negative the response, the higher level of suppression there is. The negative β weights present in the most foveal eccentricity range (0.00°–0.48°) across all visual areas are particularly prominent (especially in V1) for stimuli with steep 1/f slopes (i.e. 2.25).

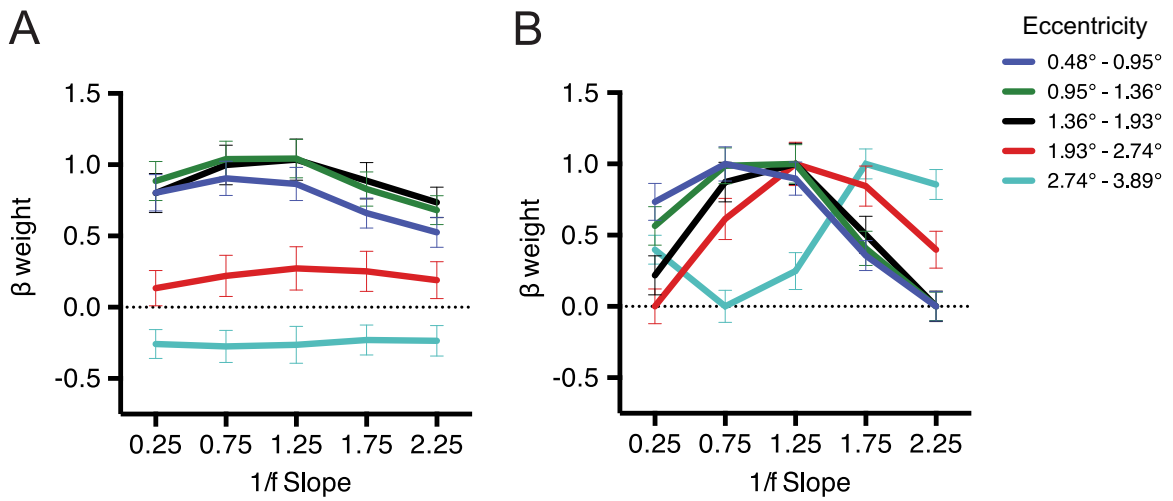

Fig. 14. Change of GLM β weights across eccentricities averaged across Experiment 1 and 2. The β weights plotted were averaged across all subjects, task conditions, contrast levels, image types and visual areas. Original β weights are depicted in (A) and normalized β weights are depicted in (B). Error bars depict SEM between subjects. The data depicted in (B) were normalized by scaling each β weight depicted in (A) between 0 and 1 within each eccentricity range.

These responses correspond with the fact that foveal eccentricity ranges are most sensitive to high SFs whereas steep 1/f slopes have low power in the high SF domain (Henriksson et al., 2008; Singh et al., 2000; Tong et al., 2012). We also observe negative β weights in the peripheral eccentricity ranges of our analysis (1.93°–3.89°). This is in line with previous work investigating the negative BOLD response (Wade and Rowland, 2010), whereby eccentricity ranges between 1.50°–3.00° have suppressed responses with high contrast foveal stimulation. Also, it has been shown that in central fixation tasks, responses in more peripheral eccentricity ranges have decreased positive BOLD response amplitude and increased negative BOLD response amplitude (Bressler et al., 2013).

There was also a significant eccentricity by task interaction (Exp 1: $F_{2.537,17.762}$=15.713, p=0.000; Exp 2: $F_{2.347,18.776}$=4.649, p=0.019). In most visual areas (particularly V3), between the AR task and the CVS task, the difference in response magnitude is smallest for the most foveal eccentricity range (0.48°–0.95°), and increases systematically with increasing eccentricity up to the most peripheral eccentricity range (2.74°–3.89°) (Exp 1: Fig. 11, Exp 2: Fig. 13), which is consistent with the attentional demands of each respective task. Since the AR task required subjects to rate their overall preference to each block of stimuli, presumably visual cortex would allocate resources to process information across each eccentricity band the stimuli subtended. In contrast, the CVS task required subjects to focus on the disk present at the center of the screen (0.00°–0.50°), hence neuronal resources would be allocated preferentially to foveal information, which is reflected in the pattern of responses for the CVS task across eccentricities ranging from the fovea to the periphery (Exp 1: Fig. 11, Exp 2: Fig. 13).

Finally, there was also a significant interaction between visual area, eccentricity, and 1/f slope (Exp 1: $F_{4.569,31.984}$=2.666, p=0.044; Exp 2: $F_{4.740,37.921}$=3.775, p=0.008). As mentioned earlier, for most visual areas the shape of the BOLD response profile across 1/f slope conditions in the foveal eccentricity range peaks between 0.75 and 1.25 and appears to be asymmetric with saturated responses for 1/f slopes 0.25 and 1.25, whereas the parafoveal eccentricity range (1.36°–1.93°) appears to be more symmetric peaking at a natural 1/f slope of 1.25 (Exp 1: Fig. 11, Exp 2: Fig. 13). However, for V1 the shape of the BOLD response profile for both the foveal and parafoveal eccentricity ranges is more asymmetric and has saturated responses between 1/f slopes 0.25 and 1.25 compared to V2 and V3 (see Fig. 2 of the Supplementary Materials). This is consistent with previous research investigating the spatial tuning profiles of early visual areas as a function of eccentricity (Henriksson et al., 2008), whereby V1 is more narrow band tuned to high SFs across eccentricities ranging from the fovea to the periphery compared to V2 and V3.

4. Discussion

The present study investigated the tuning properties of early visual cortex to the $1/f^{\alpha}$ amplitude spectrum and its associated fractal properties using fMRI. We first examined the BOLD response to synthetic grayscale noise images with varying 1/f slope values across two different contrast levels (Experiment 1). We hypothesized that if the visual system is indeed tuned to a natural distribution of SFs, maximal responses should be observed for the most "natural" 1/f slope in our set (1.25) and lower response levels for steeper or shallower slopes. We subsequently examined whether the BOLD response in early visual cortex is tuned to the geometric (structural) and photometric (intensity based) properties of natural scenes by comparing the grayscale stimuli as used in the first experiment with their thresholded (black and white) counterparts (Experiment 2). We hypothesized that if the BOLD response is driven by the geometric (fractal) characteristics of natural scenes rather than their photometric characteristics, there would be no difference in the BOLD response between grayscale and thresholded images.

4.1. The tuning of early visual cortex to the $1/f^{\alpha}$ amplitude spectrum and its associated fractal properties

Conforming to our initial hypotheses, in both experiments the BOLD response profile of early visual cortex (V1, V2, and V3) resembled an inverted U-shape peaking at 1/f slope conditions within the natural range (0.75 and 1.25). We found this pattern across different tasks, contrast levels, image types, visual areas and even eccentricity ranges. The observed strong dependence of BOLD modulation across a wide range of 1/f slopes has not been demonstrated before, as most research has focused on using narrow band stimuli, analyzing responses at isolated spatial scales (Henriksson et al., 2008; Singh et al., 2000; Tong et al., 2012). As it has been shown previously that the phase of an image does not affect the BOLD response (Olman et al., 2004; Rieger et al., 2013), we argue that using synthetic broadband noise as stimuli provided a more controlled experimental setup, yet our findings are readily applicable to actual images of natural scenes.

Interestingly, we did not observe any difference in the response profile between grayscale and thresholded image types. As our image analysis demonstrated, the thresholding procedure changes the dis-

tribution of SFs, and hence the 1/f slope, as measured using an FFT (Fig. 3). However, this change in 1/f slope did not affect responses in either visual area or in any task condition, suggesting that early visual cortex is indeed tuned to the geometric properties of natural scenes rather than their exact photometric properties. However, it is not immediately clear which specific geometric properties the visual system is tuned to or how this tuning could be implemented.

We speculate that fractal dimension (*D*), a measure of the density of structure across spatial scales (Mandelbrot, 1982; Spehar et al., 2003), may possibly account for our findings. Analysis of a wide variety of natural scenes revealed that while the average 1/f slope across natural scenes is between 1.2 and 1.4, there is considerable variability with 1/f slopes ranging from 0.6 to 1.6 (Burton and Moorhead, 1987; Field, 1987; Field, 1993; Field and Brady, 1997; Ruderman and Bialek, 1994; Tolhurst et al., 1992; van der Schaaf and van Hateren, 1996). There are two image properties that can account for this variability in the 1/f slope: 1) the amplitude of structure at different spatial scales and 2) the density of structure at different spatial scales (Field and Brady, 1997).

By measuring the rectified contrast spectrum (RCS) of a variety of natural scenes, Field and Brady (1997) found that the density of structure was relatively stable across natural scenes compared to the amplitude of structure which accounted for most of the variability. These two sources of variability can be considered analogous to the geometric and photometric properties of an image respectively, and given that they found that the photometric properties of an image account for most of the variance across natural scenes, one could predict that the visual system would be tuned to the geometric properties of an image since it is a more stable signal. This is evident in the stimuli used in the present study whereby grayscale and thresholded images have different measured 1/f slopes, but the same *D* (Table 1). One can also argue that the geometric properties of a scene are independent of the specific photometric properties across a range of illumination levels. Thresholding grayscale stimuli at different luminance intensity levels reveals the binary contour boundaries with the same fractal scaling characteristics (Fig. 4), see also in Spehar and Taylor (2013).

Although, it is theoretically possible that BOLD responses to thresholded equivalents of steep 1/f slopes (i.e. 2.25) are higher because their spectral characteristics are closer to that of natural scenes. It may have been the case that responses were balanced by the decreased effective contrast of our stimuli due to a lack of localised edges caused by the presence of large uniform areas. While it may be the case that such stimuli are not an optimal stimulus for visual areas with smaller receptive fields such as V1, this account is unlikely. For instance, the neural response to high SF sine-wave gratings in V1 and other early visual areas is not high (Henriksson et al., 2008) and is actually much lower than to sine wave gratings of lower SFs. Therefore, it is unlikely that increasing the high SF content (by for example, increasing the number of edges in such stimuli) would increase the neural response in early visual areas.

However, the possibility that effective contrast is dampening the response of thresholded stimuli generated from a 1/f slope of 2.25 is ultimately an empirical question. This could be tested by comparing neural responses to images that have the same fractal dimension but differ in local edge contrast, for example stimuli that have been thresholded at different levels (i.e. 20%, 40%, 60%, 80%; see Fig. 4 in the present manuscript; also see Spehar and Taylor, 2013). It has been shown that images thresholded at different levels have the same fractal dimension, but images thresholded at 50% have the most contours, and images with higher and lower threshold levels have fewer contours and decreased local contrast. If the visual system is indeed tuned to the geometric properties of an image as we claim, responses across all threshold levels should be very similar. Otherwise, if it is the effective contrast dampening responses, responses should be maximal for images thresholded at 50%, and decrease for images with higher or lower threshold levels. However, testing these alternative hypotheses is ultimately beyond the scope of the present paper.

In summary, the fractal scaling of structure across spatial scales is more stable compared to their photometric properties, which can vary dramatically under different levels of illumination. Hence, we speculate that networks of neurons in visual cortex are tuned to the geometric properties of natural scenes such as the density and fractal scaling of structure at different spatial scales (Field and Brady, 1997; Spehar and Taylor, 2013), but more research is needed to support our claims and most importantly better identify these specific properties.

4.2. Relating $1/f^{\alpha}$ and fractal tuning to current models of the visual system

In terms of relating our findings to current models in the field, the sparse coding model (Barlow, 1972; Field, 1987, 1994) predicts the opposite of our findings. The sparse coding model predicts that the most "natural" 1/f slope or fractal dimension (α=1.25, D=1.59) in our stimulus set should elicit the lowest response and any image outside this range would elicit higher responses in order to minimize metabolic cost and maximize energy efficiency. This model was also contradicted in a study of phase manipulation of natural images and its effect on the BOLD response whereby no changes in the BOLD response were observed across a variety of different phase noise levels (Rieger et al., 2013). Their initial hypothesis was that an intact natural image should elicit the lowest BOLD response, and as phase noise increases the BOLD response should increase. Rieger et al. (2013) came to the conclusion that early visual cortex is most likely shifting from a sparse code to a dense code with increasing levels of phase noise, but this shift from sparse to dense coding does not appear to affect metabolic cost. It is possible that this may also be the case in the present study. However, this conclusion cannot be stated with certainty as the link between metabolic cost and sparse coding has yet to be firmly established empirically.

A model that may potentially explain the strong dependence of the BOLD response to the $1/f^{\alpha}$ amplitude spectrum and its associated fractal properties is response equalization (Brady and Field, 1995; Field, 1987; Field and Brady, 1997). This model suggests that since the visual system has evolved in an environment with a $1/f^{\alpha}$ distribution of SFs with fractal scaling properties, in order to most optimally represent information in such an environment, all neurons would have to elicit the same response magnitude across different spatial scales.

In terms of SF tuning, since there is less energy at higher SFs across natural scenes, the sensitivity of the visual system increases proportionally with SF. This would allow for information at all spatial scales to be represented equally, maximizing signal and minimizing noise. The pooling of responses across different SF selective neurons would as such elicit lowered responses in early visual cortex to images with shallow and steep 1/f slopes (i.e. α=0 and 2), and higher responses to images that have natural 1/f slopes (i.e. α=~1.2). However, we found that the 1/f slope doesn't explicitly affect the BOLD response, but it is rather the geometric, fractal properties of our stimuli that drive responses. Since this is a more stable property across a variety of natural scenes (Field and Brady, 1997; Spehar and Taylor, 2013), response equalization would suggest that networks of neurons may be tuned to the amount of structure present across different spatial scales. In turn, these networks may respond in a way to elicit the same response magnitude across different spatial scales.

4.3. The interaction between receptive field size, $1/f^{\alpha}$ tuning, and fractal dimension as a function of eccentricity

To gain a more in depth understanding of the response profile across 1/f slopes, we also analyzed responses across different eccentricity ranges. Across both experiments we found a systematic change in the shape of the response profile as a function of 1/f slope. We suggest that the observed response profiles are the combination of two

components, firstly a tuning towards a 1/f slope within the natural range, where responses at most eccentricities peak at a 1/f slope of either 0.75 or 1.25 (Fig. 14). Secondly, an effect of eccentricity, where foveal eccentricity ranges respond stronger to 1/f slopes that contain more power in the high SF domain (Fig. 1A), and peripheral eccentricity ranges respond stronger to steeper 1/f slopes, which have more power in the low SF domain. The change in the shape of the response profile across eccentricity ranges reflects the known preference for high SFs in the fovea and low SFs in the periphery (Daniel and Whitteridge, 1961; De Valois et al., 1982; Henriksson et al., 2008; Sasaki et al., 2001; Talbot and Marshall, 1941).

The interplay of these two components explain the observed effect of eccentricity, with peak responses between 0.75 and 1.25 and less attenuation for steeper 1/f slopes in the periphery, and almost no attenuation for shallow 1/f slopes in the fovea. We also observe the same pattern when comparing responses in V1 to V2 and V3, where larger RFs (i.e. V3) respond more strongly towards steeper 1/f slopes and smaller receptive fields respond more strongly to shallower 1/f slopes (Exp 1: 11, Exp 2: Fig. 13). Despite this selective preference for different SFs across eccentricities and visual areas, responses still peak for 1/f slopes within the natural range (0.75 or 1.25) across most eccentricity ranges and areas. These results suggest that the formation of SF channels in human visual cortex has evolved to best represent the distribution of SFs present in natural scenes filtered through changing spatial resolution at each eccentricity range, and subsequently allowing maximum signal across all spatial scales of a scene (Field, 1987; Field and Brady, 1997). However, it has to be noted that we only investigated a limited range of central eccentricities (0.0° to 3.89°). Investigating a wider range of eccentricities would be useful, however the limited visual displays in MRI scanning setups makes this difficult.

The conclusions about responses across eccentricity ranges have solely focused on the 1/f slope and how this affects SF tuning. It is also important to note that we did not find any differences between our grayscale and thresholded stimuli, which have different 1/f slopes (Table 1) and hence different distributions of SFs. As stated previously, it is possible that the receptive fields of neurons are tuned to the density of structure across spatial scales (D), which is a more stable signal across a variety of natural scenes (Field and Brady, 1997; Spehar and Taylor, 2013). As such, in the context of fractal dimension, we can potentially interpret our results such that most eccentricity bands plotted in Fig. 14 (4/5) have preferential tuning toward a natural fractal dimension (D=1.50) and thus receptive fields in general could be conceptualized in terms of fractal dimension. Here foveal neurons have preference for images with a large amount of fine spatial detail (D=2.10), while peripheral neurons have preference for images with a large amount of coarse spatial detail (D=0.89).

5. Conclusions

We systematically investigated the neuronal response to broadband synthetic noise images that differ in their $1/f^{\alpha}$ amplitude spectrum and found a strong dependence of BOLD modulation across a wide range of 1/f slopes. We find that early visual cortex responds maximally to stimuli with a natural 1/f slope across task, image type, and contrast conditions as well as visual areas and even eccentricity ranges. These results provide evidence that at the cortical level the visual system is tuned to process images that share $1/f^{\alpha}$ amplitude spectra that is typical of natural scenes. Interestingly, we also find that it is in fact the geometric properties of natural scenes, as opposed to their photometric properties, that determine cortical response levels. We suggest this is because geometric, fractal properties are more ecologically relevant as they are more stable across various levels of illumination and a variety of natural scenes compared to photometric properties. Finally, we find that the 1/f tuning we observe interacts with the well known changes in receptive field sizes across eccentricities and visual areas. Despite a change in weighting towards higher or lower SFs and an accordant change in the shape of the tuning curve dependent on eccentricity, most eccentricity ranges we tested in early visual cortex respond maximally to natural $1/f^{\alpha}$ spectra and fractal scaling.

Acknowledgements

We thank Kevin Aquino, Alexander Puckett, Ruth Png, and Harriet Taylor for technical contributions. We also thank Colin Clifford for his advice and assistance with stimuli generation and analysis. This research was supported by Australian Research Council (ARC) grant DP120103659 to BS.

Appendix A. Supplementary material

Supplementary data associated with this article can be found in the online version at http://dx.doi.org/10.1016/j.neuroimage.2016.10.013.

References

Barlow, H.B., 1972. Single units and sensation: a neuron doctrine for perceptual psychology? Perception 1, 371–394.
Benson, N.C., Butt, O.H., Brainard, D.H., Aguirre, G.K., 2014. Correction of distortion in flattened representations of the cortical surface allows prediction of V1-V3 functional organization from anatomy. PLoS Comput. Biol. 10, e1003538.
Benson, N.C., Butt, O.H., Datta, R., Radoeva, P.D., Brainard, D.H., Aguirre, G.K., 2012. The retinotopic organization of striate cortex is well predicted by surface topology. Curr. Biol. 22, 2081–2085.
Boynton, G.M., Engel, S.A., Glover, G.H., Heeger, D.J., 1996. Linear systems analysis of functional magnetic resonance imaging in human V1. J. Neurosci. 16, 4207–4221.
Brady, N., Field, D.J., 1995. What's constant in contrast constancy? The effects of scaling on the perceived contrast of bandpass patterns. Vision. Res 35, 739–756.
Brainard, D.H., 1997. The psychophysics toolbox. Spat. Vis. 10, 433–436.
Braun, J., 1994. Visual search among items of different salience: removal of visual attention mimics a lesion in extrastriate area V4. J. Neurosci. 14, 554–567.
Brefczynski, J.A., DeYoe, E.A., 1999. A physiological correlate of the'spotlight'of visual attention. Nat. Neurosci. 2, 370–374.
Bressler, D.W., Fortenbaugh, F.C., Robertson, L.C., Silver, M.A., 2013. Visual spatial attention enhances the amplitude of positive and negative fMRI responses to visual stimulation in an eccentricity-dependent manner. Vision. Res 85, 104–112.
Buracas, G.T., Boynton, G.M., 2007. The effect of spatial attention on contrast response functions in human visual cortex. J Neurosci. 27, 93–97.
Burton, G.J., Moorhead, I.R., 1987. Color and spatial structure in natural scenes. Appl. Opt. 26, 157–170.
Chawla, D., Rees, G., Friston, K., 1999. The physiological basis of attentional modulation in extrastriate visual areas. Nat. Neurosci. 2, 671–676.
Daniel, P., Whitteridge, D., 1961. The representation of the visual field on the cerebral cortex in monkeys. J Physiol. 159, 203–221.
De Valois, R.L., Albrecht, D.G., Thorell, L.G., 1982. Spatial frequency selectivity of cells in macaque visual cortex. Vision. Res 22, 545–559.
Field, D.J., 1987. Relations between the statistics of natural images and the response properties of cortical cells. J. Opt. Soc. Am. A 4, 2379–2394.
Field, D.J., 1993. Scale-invariance and self-similar "wavelet" transforms: an analysis of natural scenes and mammalian visual systems. In: Farfe, M., Hunt, J., Vassilicos, J.C. (Eds.), Wavelets, fractals and Fourier transforms. Oxford University Press, Oxford.
Field, D.J., 1994. What is the goal of sensory coding? Neural Comput. 6, 559–601.
Field, D.J., Brady, N., 1997. Visual sensitivity, blur and the sources of variability in the amplitude spectra of natural scenes. Vision. Res. 37, 3367–3383.
Fischl, B., Dale, A.M., 2000. Measuring the thickness of the human cerebral cortex from magnetic resonance images. Proc. Natl. Acad. Sci. USA 97, 11050–11055.
Fischl, B., Sereno, M.I., Tootell, R.B., Dale, A.M., 1999. High-resolution intersubject averaging and a coordinate system for the cortical surface. Hum. Brain Mapp. 8, 272–284.
Grill-Spector, K., Kushnir, T., Edelman, S., Avidan, G., Itzchak, Y., Malach, R., 1999. Differential processing of objects under various viewing conditions in the human lateral occipital complex. Neuron 24, 187–203.
Hansen, B.C., Hess, R.F., 2006. Discrimination of amplitude spectrum slope in the fovea and parafovea and the local amplitude distributions of natural scene imagery. J. Vis. 6, 696–711.
Henriksson, L., Nurminen, L., Hyvarinen, A., Vanni, S., 2008. Spatial frequency tuning in human retinotopic visual areas. J. Vis. 8, [5.1–13].
Juricevic, I., Land, L., Wilkins, A., Webster, M.A., 2010. Visual discomfort and natural image statistics. Perception 39, 884.
Kanwisher, N., McDermott, J., Chun, M.M., 1997. The fusiform face area: a module in human extrastriate cortex specialized for face perception. J. Neurosci. 17, 4302–4311.
Kastner, S., Pinsk, M.A., De Weerd, P., Desimone, R., Ungerleider, L.G., 1999. Increased activity in human visual cortex during directed attention in the absence of visual stimulation. Neuron 22, 751–761.

Knill, D.C., Field, D., Kersten, D., 1990. Human discrimination of fractal images. J. Opt. Soc. Am. A 7, 1113–1123.
Laron, M., Cheng, H., Zhang, B., Frishman, L.J., 2009. The effect of eccentricity on the contrast response function of multifocal visual evoked potentials (mfVEPs). Vision. Res. 49, 1711–1716.
Legge, G.E., Kersten, D., 1987. Contrast discrimination in peripheral vision. J. Opt. Soc. Am. A 4, 1594–1598.
Lindquist, M.A., 2008. The statistical analysis of fMRI data. Stat. Sci. 23, 439–464.
Liu, T., Pestilli, F., Carrasco, M., 2005. Transient attention enhances perceptual performance and fMRI response in human visual cortex. Neuron 45, 469–477.
Mandelbrot, B.B., 1982. The Fractal Geometry of Nature. W.H. Freeman and Company, New York.
McDonald, J.S., Tadmor, Y., 2006. The perceived contrast of texture patches embedded in natural images. Vision. Res. 46, 3098–3104.
Olman, C.A., Ugurbil, K., Schrater, P., Kersten, D., 2004. BOLD fMRI and psychophysical measurements of contrast response to broadband images. Vision. Res. 44, 669–683.
Pelli, D.G., 1997. The VideoToolbox software for visual psychophysics: transforming numbers into movies. Spat. Vis. 10, 437–442.
Rieger, J.W., Gegenfurtner, K.R., Schalk, F., Koechy, N., Heinze, H.J., Grueschow, M., 2013. BOLD responses in human V1 to local structure in natural scenes: implications for theories of visual coding. J. Vis. 13, 19.
Rikhye, R.V., Sur, M., 2015. Spatial correlations in natural scenes modulate response reliability in mouse visual cortex. J. Neurosci. 35, 14661–14680.
Ruderman, D., Bialek, W., 1994. Statistics of natural images: scaling in the woods. Phys. Rev. Lett. 73, 814–817.
Salat, D.H., Buckner, R.L., Snyder, A.Z., Greve, D.N., Desikan, R.S., Busa, E., Morris, J.C., Dale, A.M., Fischl, B., 2004. Thinning of the cerebral cortex in aging. Cereb. Cortex 14, 721–730.
Sasaki, Y., Hadjikhani, N., Fischl, B., Liu, A.K., Marrett, S., Dale, A.M., Tootell, R.B., 2001. Local and global attention are mapped retinotopically in human occipital cortex. Proc. Natl. Acad. Sci. USA 98, 2077–2082.
Schira, M.M., Spehar, B., 2011. Differential effect of contrast polarity reversals in closed squares and open L-Junctions. Front Psychol., 2.
Schira, M.M., Wade, A.R., Tyler, C.W., 2007. Two-dimensional mapping of the central and parafoveal visual field to human visual cortex. J. Neurophysiol. 97, 4284–4295.
Schira, M.M., Tyler, C.W., Breakspear, M., Spehar, B., 2009. The foveal confluence in human visual cortex. J. Neurosci. 29, 9050–9058.
Singh, K.D., Smith, A.T., Greenlee, M.W., 2000. Spatiotemporal frequency and direction sensitivities of human visual areas measured using fMRI. Neuroimage 12, 550–564.
Spehar, B., Taylor, R.P., 2013. Fractals in art and nature: why do we like them?, IS & T/SPIE Electronic Imaging. Int. Soc. Opt. Photonics, [865118-865118-865112].
Spehar, B., Clifford, C.W.G., Newell, B.R., Taylor, R.P., 2003. Universal aesthetic of fractals. Comput. Graph. 27, 813–820.
Spehar, B., Wong, S., van de Klundert, S., Lui, J., Clifford, C.W., Taylor, R.P., 2015. Beauty and the beholder: the role of visual sensitivity in visual preference. Front Hum. Neurosci., 9.
Tadmor, Y., Tolhurst, D.J., 1994. Discrimination of changes in the second-order statistics of natural and synthetic images. Vision. Res. 34, 541–554.
Talbot, S., Marshall, W., 1941. Physiological studies on neural mechanisms of visual localization and discrimination. Am. J. Ophthalmol. 24, 1255–1264.
Tolhurst, D.J., Tadmor, Y., Chao, T., 1992. Amplitude spectra of natural images. Ophthalmic Physiol. Opt. 12, 229–232.
Tong, F., Harrison, S.A., Dewey, J.A., Kamitani, Y., 2012. Relationship between BOLD amplitude and pattern classification of orientation-selective activity in the human visual cortex. Neuroimage 63, 1212–1222.
Tootell, R.B., 1995. Visual motion aftereffect in human cortical area MT revealed by functional magnetic resonance imaging. Nature 375, 139–141.
Tootell, R.B., Hadjikhani, N., Hall, E.K., Marrett, S., Vanduffel, W., Vaughan, J.T., Dale, A.M., 1998. The retinotopy of visual spatial attention. Neuron 21, 1409–1422.
van der Schaaf, A., van Hateren, J.H., 1996. Modelling the power spectra of natural images: statistics and information. Vision. Res. 36, 2759–2770.
Wade, A.R., Rowland, J., 2010. Early suppressive mechanisms and the negative blood oxygenation level-dependent response in human visual cortex. J. Neurosci. 30, 5008–5019.
Willenbockel, V., Sadr, J., Fiset, D., Horne, G.O., Gosselin, F., Tanaka, J.W., 2010. Controlling low-level image properties: the SHINE toolbox. Behav. Res Method. 42, 671–684.
Xing, Y., Ledgeway, T., McGraw, P.V., Schluppeck, D., 2013. Decoding working memory of stimulus contrast in early visual cortex. J. Neurosci. 33, 10301–10311.